nature materials

SUPPLEMENTARY INFORMATION

DOI: 10.1038/NMAT3455

Design of zeolite by inverse sigma transformation

Table of Contents

DOI: 10.1038/NMAT3455

Methods

Synthesis

Template synthesis

Preparation of the structure direction agent (SDA), (6*R*,10*S*)-6,10-dimethyl-5-azoniaspiro[4,5]decane hydroxide, was done according to reference1. In a 500 mL round bottom flask 5.68 g NaOH (Aldrich) and 30.66 g 1,4-dibromobutane (Aldrich) were dissolved in 140 mL deionized water. Subsequently 16.07 g (2R,6S)-2,6-dimethylpiperidine (Aldrich) was added and the mixture heated to boiling temperature under reflux and intensive stirring overnight. Afterwards the solution was cooled in an ice bath. 70 mL ice cooled 50 wt% NaOH solution was added, and subsequently another 20 g of solid NaOH. Intensive stirring of the mixture at 0 °C led to crystallization of the SDA. The SDA product was filtered and residual water removed via extraction with 100 mL chloroform, a procedure that was repeated twice. The chloroform was evaporated to a residual volume of 100 mL and the bromide salt precipitated with diethylether. Finally the bromide was converted to hydroxide by ion exchange with Dowex SBR LCNG resin for 48 hours. The successful synthesis of the template was confirmed by ^{1}H-NMR and ^{13}C-NMR. The aqueous solution of SDA was concentrated to 20-30 wt% typically by evaporation under reduced pressure in a rotary evaporator.

IM-12 zeolite synthesis

IM-12 zeolite was synthesized using the procedure of reference 1. A reaction mixture with molar oxide composition of 0.75 SDA : GeO_2 : 2 SiO_2 : 75 H_2O was prepared from 2.78 g tetraethylorthosilicate (TEOS) (Aldrich), 0.70 g crystalline GeO_2 (Aldrich) and the adequate quantity of SDA solution and water. First GeO_2 was dissolved in the mixture of SDA and water in a 60 mL polypropylene bottle. TEOS was slowly added and the resulting mixture stirred at room temperature for 40 min in the sealed bottle. The resulting mixture was transferred in a Teflon-lined stainless steel autoclave and heated for 6 days at 175 °C under agitation (tumbling autoclaves). The solids were recovered by filtration, washed with deionized water and dried overnight at 60 °C. The as-synthesized IM-12 was calcined for 6 hours at 550 °C in a muffle furnace using a temperature ramp of 1 °C/min.

Characterisation

Powder diffraction

X-ray powder diffraction data of -COK-14 dried at 60°C and the fully connected sample COK-14 were recorded on a STOE Stadi MP diffractometer with focusing Ge(111) monochromator (Cu$K\alpha_1$ radiation, λ = 1.54056 Å) in Debye-Scherrer geometry with a linear position sensitive detector (PSD) (6 °2θ window) from 4 to 90 °2θ, with a step width of 0.5 degree, internal PSD resolution of 0.01 degree, and a steptime of 250s. The samples were continuously rotated in a 0.5 mm glass capillary (Hilgenberg) to improve statistics. Measurements occurred at room temperature.

X-ray powder diffraction experiments on -COK-14 equilibrated with ambient humidity were performed at the B2 beamline at DESY (*Deutsches Elektronensynchrotron*) in Hamburg, Germany[2] with a position sensitive image

plate detector (OBI, *ortsfest auslesbarer Bildplattendetektor*)[3] at the germanium K-edge (11.1keV) in transmission geometry. To improve statistics, the samples were continuously rotated in a 0.5 mm glass capillary. High resolution Powder X-ray diffraction data for Ge-COK-14 material were collected at room temperature at the Swiss Norwegian Beamline (SNBL, BM01B[4]) in collaboration with the DUBBLE beamline at the European Synchrotron Radiation Facility (ESRF, Grenoble). The beamline was set to a wavelength of λ = 0.50240(9) Å. by a Si (111) channel-cut monochromator. A 1.0 mm glass capillary (Hilgenberg) containing the sample was spun during data collection to minimize preferred orientation phenomena. Data were collected in continuous mode over the range 1.0 – 55.5 °2θ (accumulation time increased with increasing scattering angle) and were rebinned with a step size of 0.003 °2θ. 10 scans were collected and summed to increase the signal to noise ratio. Rietveld refinements on all powder diffraction data were performed using the GSAS/EXPGUI software[5,6].

EXAFS

The X-ray absorption spectra for Ge-COK-14 material were collected at room temperature at the Dutch-Belgian Beamline (DUBBLE[7]) and at the Swiss Norwegian Beamline (SNBL, BM01B) at the European Synchrotron Radiation Facility (ESRF, Grenoble) using Si (111) double crystal monochromator. The Ge K-edge XAS were measured in transmission and continuous scanning mode from 11000 eV to 12500 eVwith the step of 1eV for 5min. The sample was measured in a 1.0 mm glass capillary (Hilgenberg). Several scans were collected and summed to increase the signal to noise ratio. All data treatment and analysis was performed using the Athena and Artemis packages[8] of the IFEFFIT[9] programming interface Demeter[10] in combination with FEFF6[11] calculations yielding theoretical phase shifts and amplitudes. The EXAFS analysis was performed by concurrently fitting k^1, k^2 and k^3 weighted data in in k-space.

NMR

All ^{29}Si MAS NMR spectra were recorded on a Bruker AMX300 spectrometer (7.0 T). At this field, the resonance frequency of ^{29}Si was 59.6 MHz. 4000 scans were accumulated with a recycle delay of 60 s. The pulse length was 5.0 µs. The samples were packed in 4 mm zirconia rotors. The spinning frequency of the rotor was 5000 Hz. Tetramethylsilane was used as chemical shift reference. The spectra were de-convoluted assuming Gaussian shape of the NMR signals, using the Igor software[12].

Two samples were analyzed by ^{1}H solid state resolution NMR: Ge-COK-14 and –COK-14. For both MAS NMR and homo-decoupled MAS NMR using windowless PMLG pulse sequence were used. The ^{1}H NMR spectra were recorded on an Avance III Bruker 200 spectrometer at a MAS frequency of 5 kHz. The ^{1}H Hahn-echo (90º-180º-90º) spectra were acquired using a 3.1 ms 90º pulse length and inter-pulse delays synchronized with one rotor period. ^{1}H NMR spectra were also recorded using the windowed phase modulated Lee-Goldburg[13,14] (*w*PMLG) sequence to remove the ^{1}H-^{1}H homonuclear dipolar couplings. The *w*PMLG[15] version was used with an acquisition window of 4.5 ms, and RF field of *ca.* 100 kHz. For each spectrum, 64 transients were accumulated, with 5 s recycle delay. The ^{1}H chemical shifts were referenced to TMS. The spectra were reconstructed using the Dmfit[16] software.

DOI: 10.1038/NMAT3455

TGA

Thermal gravimetric analysis was performed on a TGA Q500 (TA instruments, Belgium) under nitrogen flow at a heating rate of 1 °C min^{-1} until 900°C.

Element analysis

Determination of the Si and Ge content of the samples was measured with ICP performed on a Optima 4300 DV2 (Perkin Elmer). 100 mg of -COK-14 and 500 mg $LiBO_2$ were homogenized and transferred in a graphite plate. This was placed for 15 minutes in a muffle furnace at 1000°C. Subsequently 50 mL of a 0.42 M HNO_3 solution was added and the mixture remained stirring for 15 minutes. 10 mL was transferred in a separate bottle. After 24h, the remaining graphite was precipitated.

Nitrogen adsorption

Nitrogen adsorption isotherms at -196 °C were recorded on an Autosorb-1 instrument (Quantachrome, USA). The samples were evacuated at 250 °C under vacuum for 12 h. The specific surface area and micropore distribution were determined using the BET method and the SF analysis[17], respectively. The external surface area and micropore volume were determined using the t-plot method.

TEM analysis

TEM images were recorded with a FEI CM30 microscope, operated at 300 kV, high magnification images using a FEI Tecnai G2 microscope, operated at 200 kV. Diffraction patterns were recorded using a FEI CM20 microscope, operated at 200 kV.

Computational details

Forcefield calculations

All forcefield calculations were performed using the Gulp program[18] with the parameters of the Catlow library[19]. Forcefield calculation served to roughly assess framework stability and served as input for the Rietveld refinements of -COK-14 and COK-14. Ge-COK-14 was not simulated as no suitable forcefield parameters were available.

DFT

DFT calculations were performed with the periodic DFT code VASP (Vienna Ab initio Simulation Package)[20,21]. This code uses projector-augmented waves and a plane wave basis set to describe the electron density. The exchange-correlation functional is expressed by the generalized-gradient approximation with the Perdew-Burke-Ernzerhof parameterization.

As the unit cell is relatively large, a gamma point sampling of the reciprocal space suffices. Calculations are spin polarized with a plane wave cut-off energy 600 eV. Electronic convergence was set to 10^{-5} and geometries are converged to 0.05 eV/Å. Van der Waals corrections are included adding empirical corrections as proposed by Grimme[22]. Energies refer to ground energies and do not account for thermal corrections.

All calculations start from the provided experimental data. Hydrogen atoms were added to the zeolite to obtain properly terminated structures. For the calculations on structures including water molecules we started random orientation for water molecules to avoid starting close to a local minimum. All cell parameters were systematically relaxed.

Structure determination

Structure determination of -COK-14

The diffraction pattern of -COK-14 retained several reflections of the IM-12 parent material (Fig. 2, main document) but could not be indexed in the same unit cell. This clearly marked it as new crystalline material structurally related to IM-12. Indexing of the powder pattern resulted in a unit cell of a = 24.64 Å, b = 13.92 Å, c = 12.26 Å and a monoclinic angle of 109.20° with as possible space group C 2/m. Space group and lattice constants were fully confirmed by TEM (Fig. S1).

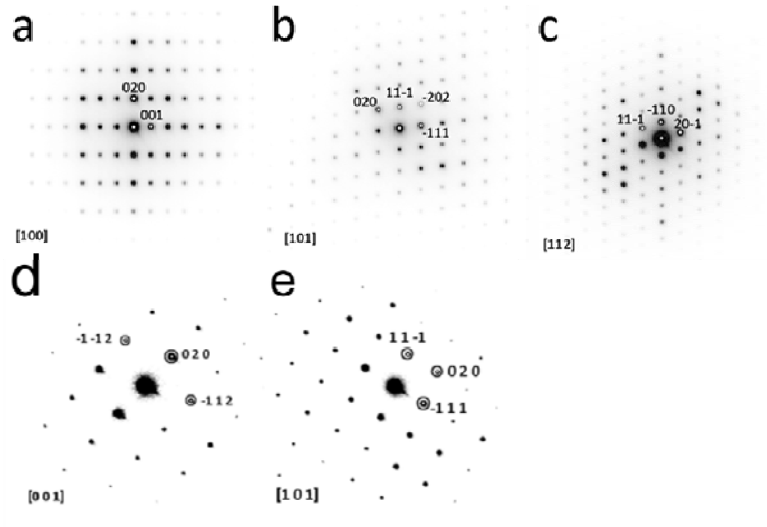

Figure S1 : Electron diffraction patterns of (a, b and c) three different zone axes of the stacked sheets of –COK-14. D and e show corresponding patterns of the IM-12 parent material confirming similar dimensions in the *bc*-plane but a different distance in the *a* direction. See inserts in Fig. 2, main document for morphology.

The *b* and *c* lattice parameters of -COK-14 very closely resembled the corresponding constants of the IM-12 structure (a = 29.00 Å, b = 13.98 Å c = 12.45 Å, β = 104.91°)[23], but the *a* direction was found to be significantly shorter. The *bc*-planes in IM-12 are parallel to the layers so it was a straightforward conclusion in the new structure these layers were partially or fully preserved but stacked in a different way. Through coordinate transformation of the atomic positions of the IM-12 framework, the layers were translated into the new unit cell and the connecting cubes were removed. The new coordinates served as input for an initial refinement, with strongly constrained bond angles and distances for the silicate tetrahedra. Refinement of the unit cell turned out to be quite stable but reflection intensities could not satisfactorily be reproduced, as in this starting model the layers were not yet connected. A search of the electron density maps showed clear electron density between the layers, in a position corresponding to the location of D4R in the IM-12 zeolite. To explore in more detail how the layers are connected in -COK-14, a SiO_4 tetrahedron was placed as rigid body in the centre of the observed electron density and left to refine freely. This tetrahedron aligned precisely between the layers and connected with upper and lower layers. In the C2/m space group this led to the formation of a single 4R in place of the D4R known to connect the layers in the IM-12 material (Fig. 1, main document). With this structural concept a new set of starting parameters for refinement was calculated using GULP[18] and the Catlow forcefield[19]. A stable solution

DOI: 10.1038/NMAT3455

was found but the simulated lattice constant along *a* was by 0.5 Å too short, while the other unit cell constants were reproduced satisfactorily.

^{29}Si MAS NMR spectroscopy served to optimise the structural model (Fig. S2 and Fig. 2 main document). Considering the framework contained a significant number of silanols (11% Q^3, Table S1), the possibility of a systematically interrupted framework was explored. Comparing the model structure with the ^{29}Si MAS NMR data, the observed concentration of hydroxyls (11%) could almost exactly be generated by breaking two bonds in the 4R created by the layer linking Si-tetrahedra. This concept led to two model frameworks where the silicate layers are connected by sideways linked dimers of tetrahedra (Fig. S3a and c). Depending on the cut, these layer linking tetrahedra were condensed pairwise either in *b* or *c* direction. The models were optimized in GULP[18] where it turned out the structure with the layer linking tetrahedra condensed in *c* direction could satisfactorily be minimized in energy (Fig. S3c). This resulted in lattice parameters very close to the experimental data and with a lower framework energy compared to the fully connected starting model (Fig. S3b). The model with the layer linking tetrahedra condensed in *b* direction could not successfully be optimized and yielded unit cell values that strongly deviate from the experimental values (Fig. S3a).

Table S1 : Parameters obtained by fitting ^{29}Si MAS NMR spectra shown in Fig. S2. As fitting profiles Gaussians were chosen.

Sample	**Q^3**		**Q^4-nGe**		**Q^4-4Si**	
	Shift (ppm)	Intensity (%)	Shift (ppm)	Intensity (%)	Shift (ppm)	Intensity (%)
IM-12	-99.6	3.6	-106.4	38.2	-113.5 -111.4	50.4 7.8
Ge-COK-14	-101.7	17.6	-107.2	9.5	-112.7 -111.4	67.2 5.8
-COK-14	-100.9	11			-110.7	89

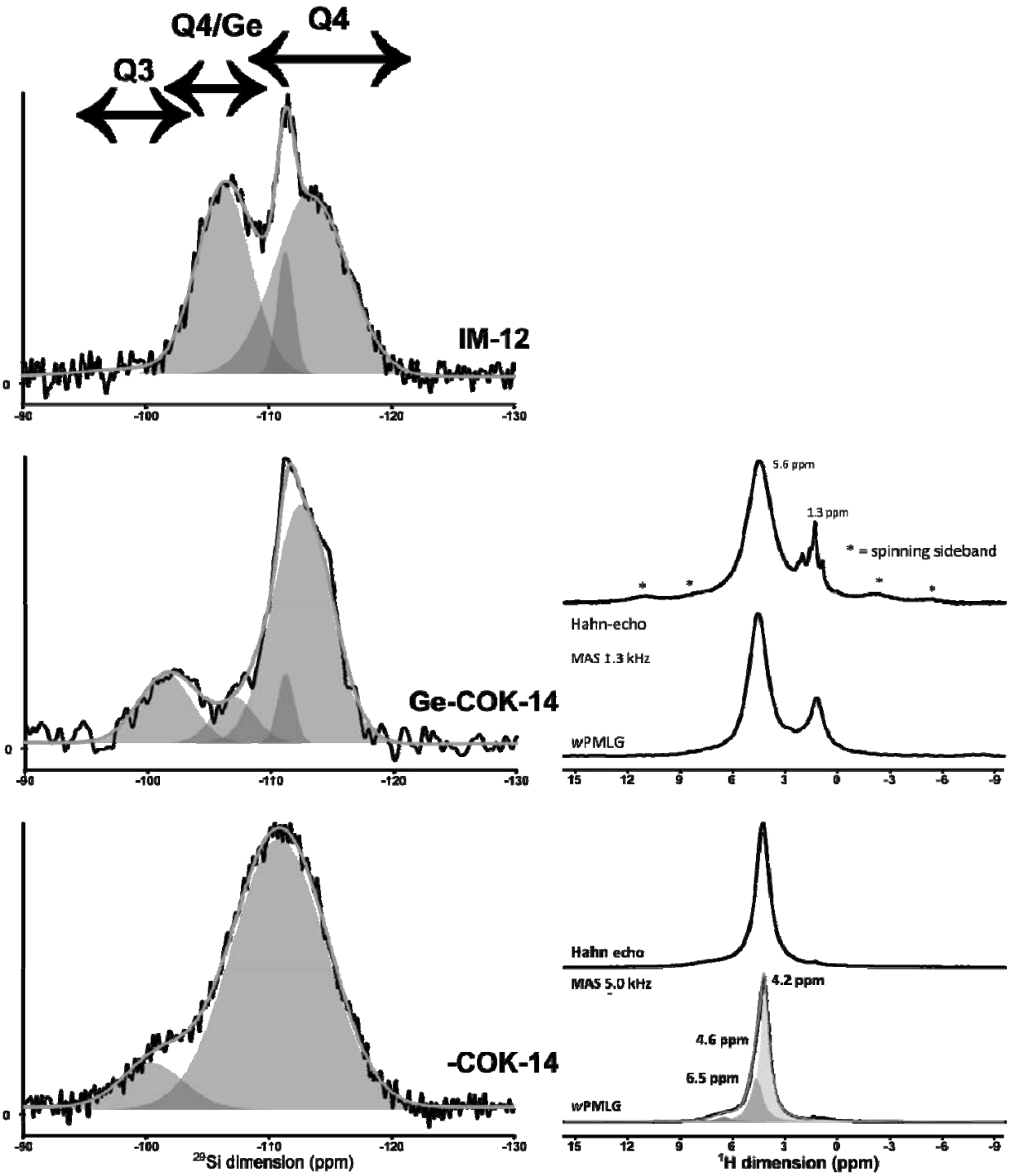

Figure S2 : NMR spectra of IM-12 (top), Ge-COK-14 (middle), and –COK-14 (bottom). Left: ^{29}Si-spectra. Regions allocated to different Si-environments are indicated. Right: ^{1}H MAS and wPMLG spectra

DOI: 10.1038/NMAT3455

Additional confirmation of the proposed model with the layer linking tetrahedra condensed in *c* direction (Fig. S3c) was obtained by performing high level Density Functional Theory (DFT) calculations. This led to a very good reproduction of the lattice constants (a = 25.1 Å, b = 14.2 Å c = 12.5 Å, β = 109°) and, indeed, the predicted break of the 4R into dimers. As already suggested by the forcefield calculations and Rietveld refinement, DFT fully confirmed that the hydroxyl groups, generated by breaking each 4R, point outwards into the 12 membered ring (Fig. S3c). With Rietveld refinement the presence of a strained angle between Si_4-O_6-Si_4 of 180° was noticed and this was confirmed by the DFT calculations, even in lowest possible symmetry P1. This suggests the space group C2/m to be the true symmetry of this material.

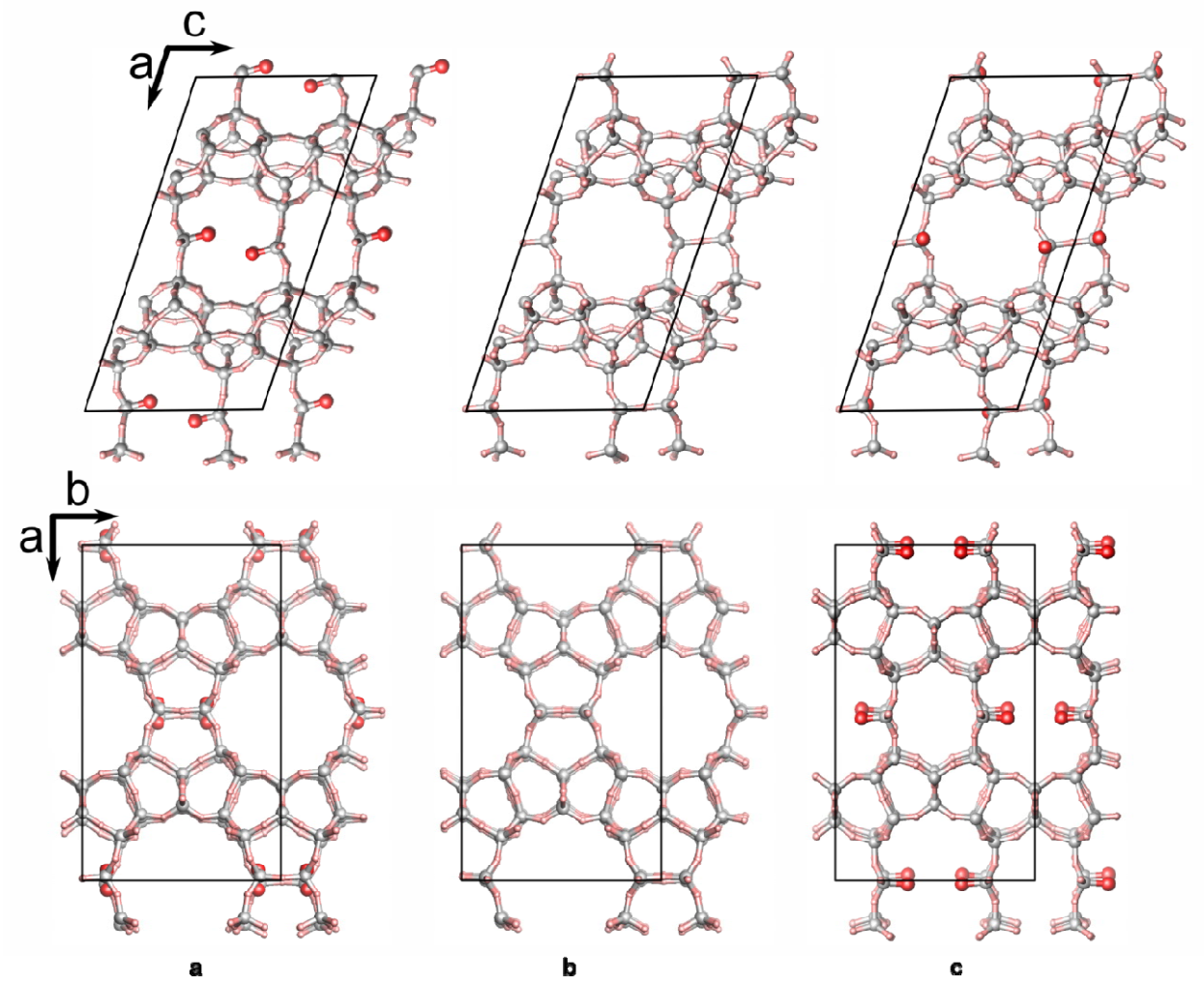

Figure S3 : Linking of silicate layers in possible framework structures of -COK-14: (a) layer linking tetrahedra condensed pairwise in the *b* direction; (b) fully connected framework and (c) layer linking tetrahedra condensed pairwise in the *c* direction.

Rietveld refinement of the structure (Fig. 3, left, main document) with this new set of parameters revealed electron density between the hydroxyls, which were identified as bridging water molecules and included in the refinement. At later stages, further electron density was assigned to water and freely refined. At the same time, bond angle and distance restraints of the framework were successively lowered to a weighing of 0.2. This led to

the description of a hydrogen-bonded water structure stabilized by interaction with framework silanol groups. To further verify if the structure solution was correct, a Rietveld refinement of synchrotron data collected at B2 beamline at the Hasylab in Hamburg was performed (Fig. S4). The investigated sample was equilibrated with ambient humidity and contained a higher number of water molecules compared to the partially dried sample. Fig. 3, left in the main document and Fig. S4 show the experimental and simulated XRD patterns of -COK-14 as well as the difference profiles[24]. The proposed interrupted framework structure of -COK-14 was hereby fully confirmed. Lattice constants, R-values and bond angles and distances can be found in Table S2. The entire list of coordinates, can be found in appended Tables S8 – S10. In full agreement the material showed a porosity typical for zeolites with a pore-size comparable to FAU zeolite[23], indicating the presence of 12-ring channels (Fig. S5, Table S3). The structure solution of -COK-14 revealed a systematically broken framework with pairs of neighbouring silanol groups. DFT calculations and FTIR on –COK-14 and its deuterated form (Fig. S6) revealed these silanol-groups are stable even at elevated temperatures up to 300°C and are in interaction with hydrogen bonded water molecules. This conclusion also is strongly supported by ^{1}H-NMR (Fig. S2). For –COK-14, MAS only spectrum, a signal at about 4.4 ppm is observed as the sum of resonances centered at 4.2 and 4.6 ppm. In addition a residual signal at 6.5 ppm is detected. The two former resonances can be assigned to water at 4.6 ppm while the 4.2 ppm is assigned to silanols strongly associated to water[25]. The protons of this ensemble are in fast exchange and appear at the weighted averaged value of isolated silanol and isolated water. However, thermogravimetry (Fig. S7) suggested at temperatures above 300°C these exceptionally strongly bound water molecules are released and the silanol groups condense which results in the fully connected framework of COK-14.

In earlier work by Roth *et al.* a B-UTL has been treated under milder acid condtions (0.1M HCl)[26]. A material called ICP-1P was interpreted as a lamellar material after degradation of the double four-rings. Stabilization with $Si(CH_3)_3(OCH_2CH_3)_2$ resulted in a material named IPC-2, referring to an interlamellar expanded zeolite. In this manuscript it is shown that a more severe acidic treatment directly leads to a 3D material, -COK-14.

DOI: 10.1038/NMAT3455

Table S2 : Lattice constants, R-values and bond distances and angles of the refined and simulated –COK-14. Rietveld refinement occurred in the space group C 2/m and simulation in P1, but resulted in coordinates agreeing with the monoclinic space group used for refinement.

		a (Å)	*b (Å)*	*c (Å)*	*β (°)*
-COK-14 ambient humidity	lattice parameters	24.6355(10)	13.93666(23)	12.2637(4)	109.2189(33)
	estimated standard deviation in brackets				
	Radiation	***λ (Å)***	**R-values (%)**		
	synchrotron	1.1172	Rp	2.6	
			Rwp	3.3	
			RF^2	8.8	
	Bond	**Distance (Å)**	**Bond**	**Distance (Å)**	
	Average Si – Si	3.085	Average Si – O	1.609	
	Minimum Si – Si	2.96	Minimum Si – O	1.567	
	Maximum Si – Si	3.18	Maximum Si – O	1.624	
	Bond	**Angle (°)**	**Bond**	**Angle (°)**	
	Average Si – O – Si	153.7	Average O – Si – O	109.5	
	Minimum Si – O – Si	134.5	Minimum O – Si – O	103.4	
	Maximum Si – O – Si	180	Maximum O – Si – O	114.5	
		a (Å)	***b (Å)***	***c (Å)***	***β (°)***
-COK-14 dried at 60C	lattice parameters	24.6406(6)	13.92386(21)	12.25976(28)	109.1961(21)
	estimated standard deviation in brackets				
	Radiation	***λ (Å)***	**R-values (%)**		
	$Cu_{K\alpha 1}$	1.54056	Rp	3.2	
			Rwp	4.5	
			RF^2	11.4	
	Bond	**Distance (Å)**	**Bond**	**Distance (Å)**	
	Average Si – Si	3.072	Average Si – O	1.599	
	Minimum Si – Si	2.883	Minimum Si – O	1.553	
	Maximum Si – Si	3.192	Maximum Si – O	1.651	
	Bond	**Angle (°)**	**Bond**	**Angle (°)**	
	Average Si – O – Si	151.46	Average O – Si – O	109.452	
	Minimum Si – O – Si	126.63	Minimum O – Si – O	105.23	
	Maximum Si – O – Si	180	Maximum O – Si – O	113.98	
		a (Å)	***b (Å)***	***c (Å)***	***β (°)***
-COK-14 DFT	lattice parameters	25.1	14.2	12.5	109
	Bond	**Distance (Å)**	**Bond**	**Distance (Å)**	
	Si - Si	3.087	Si – O	1.619	
	Bond	**Angle (°)**	**Bond**	**Angle (°)**	
	Si – O – Si	154.178	O – Si – O	109.469	

Table S3 : Surface area and porosity of -COK-14 and IM-12 zeolite according to nitrogen adsorption measurements.

	-COK-14	IM-12
BET surface area (m^2/g)	406	431
External surface area (m^2/g)	54	9
Micropore volume (cm^3/g)	0.190	0.212
Pore size[17] (Å)	7.6	9.5

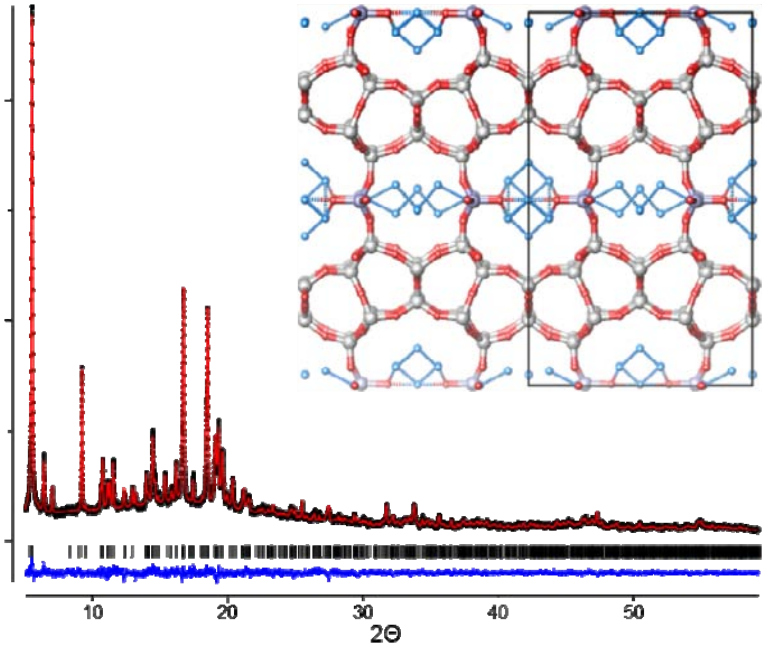

Figure S4 : Rietveld refinement of -COK-14 equilibrated with ambient humidity, recorded using synchrotron radiation (λ = 1.1172 Å). Experimental (black) and calculated (red) XRD patterns as well as their difference profile are shown (blue). The short tick marks below the patterns give the position of the Bragg reflections.

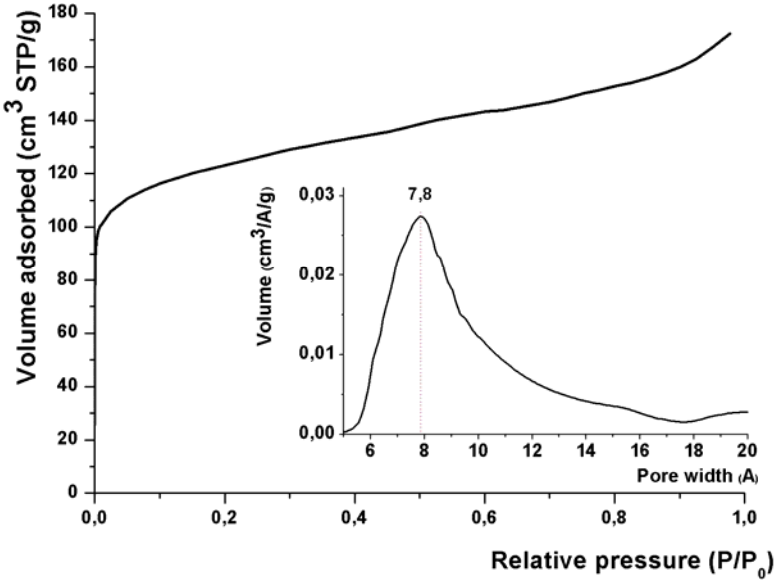

Figure S5 : Nitrogen adsorption isotherm of -COK-14 zeolite. The insert shows the micropore distribution (SF method[17]). -COK-14 zeolite is characterized by pores with a width of 7.8 Å (Table S3).

DOI: 10.1038/NMAT3455

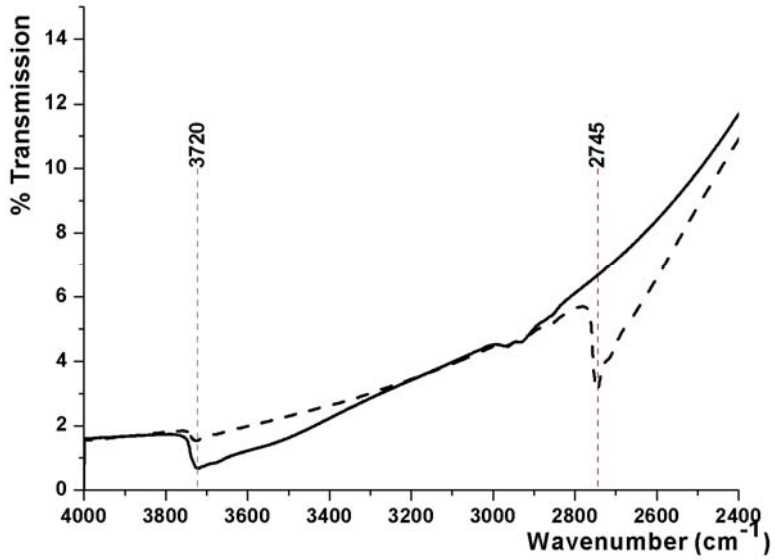

Figure S6 : FTIR spectra recorded at 300 °C of –COK-14 (straight line) and deuterated -COK-14(D) (dashed line). The signal at 3720 cm^{-1} in –COK-14, assigned to isolated silanols in the interior of the zeolite[27], shifts consistently upon deuteration. The ratio of both signals is 0.738, which is in good agreement with the theoretical value of 0.727.

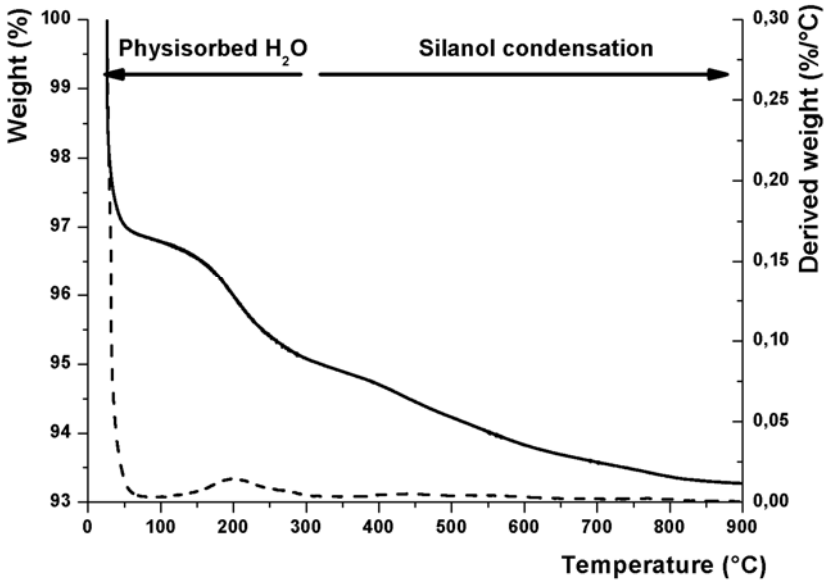

Figure S7 : TGA analysis of -COK-14. The dashed line corresponds to the derivation of weight loss. The slow and steady water loss above 300°C was interpreted as progressing silanol condensation.

Structure refinement of COK-14

TG measurements (Fig. S7) suggested the interrupted framework of –COK-14 could be transformed into a fully connected structure COK-14. To verify this was indeed the case, a sample of –COK-14 was calcined at 550 °C and transferred into a capillary for X-ray diffraction excluding all contact to humidity. As discussed in the previous section, unit cell dimensions and coordinates for a fully closed tetrahedral framework COK-14 were already obtained by forcefield calculation and these were used as a starting model for Rietveld refinement. Atom-positions were initially strongly constrained to retain tetrahedral angles and typical bond distances. The refinement very quickly converged, fully supporting the theoretical values. Towards the end of the refinement the weight of bond and angle restraints was successively lowered. However, lowering the constraint weight below 0.8 led to an instable refinement. An inspection of the obtained structure model revealed rather high temperature factors of several atoms. Especially two oxygen sites were found to have significantly shortened bonds to neighbouring Si sites: O10 and Ob with 1.56 and 1.54 Å, respectively (Table S11 for atom numbering, Table S4 for average, minimum and maximum bond distances and angles and Fig. S8 shows the specifically strained atoms). It also turned out the Si-O-Si angles for several O-atoms took unusual small values, specifically for O10, O14 and O16. Typical for all these oxygen sites is the vicinity to the connecting 4R between the layers. Significant strain in the structure also could be deduced by significant deviation of one tetrahedral angle on Si sites which directly connect to the 4R (Si6, Si7). This observation, along with the calculated low framework energy of the closed structure compared to the open –COK-14, explains why a lower weight of constraints during refinement did not succeed. On the other hand, the very good fit of experimental and simulated powder pattern (Fig. S8) and the excellent R-factors (Rp=2.08%, Rwp=2.9%, RF^2=7.4%) strongly suggest the structure indeed can exist in fully closed form if contact with water is avoided. The high sensitivity towards water was confirmed by a simple experiment. The capillary was opened and exposed to ambient. Quickly after, the X-ray pattern had returned to the original unit cell of the broken framework –COK-14. Unfortunately, no air and water tight rotors for NMR measurements were available, therefore an NMR experiment probing the silanol-content of the closed structure could not be performed.

DOI: 10.1038/NMAT3455

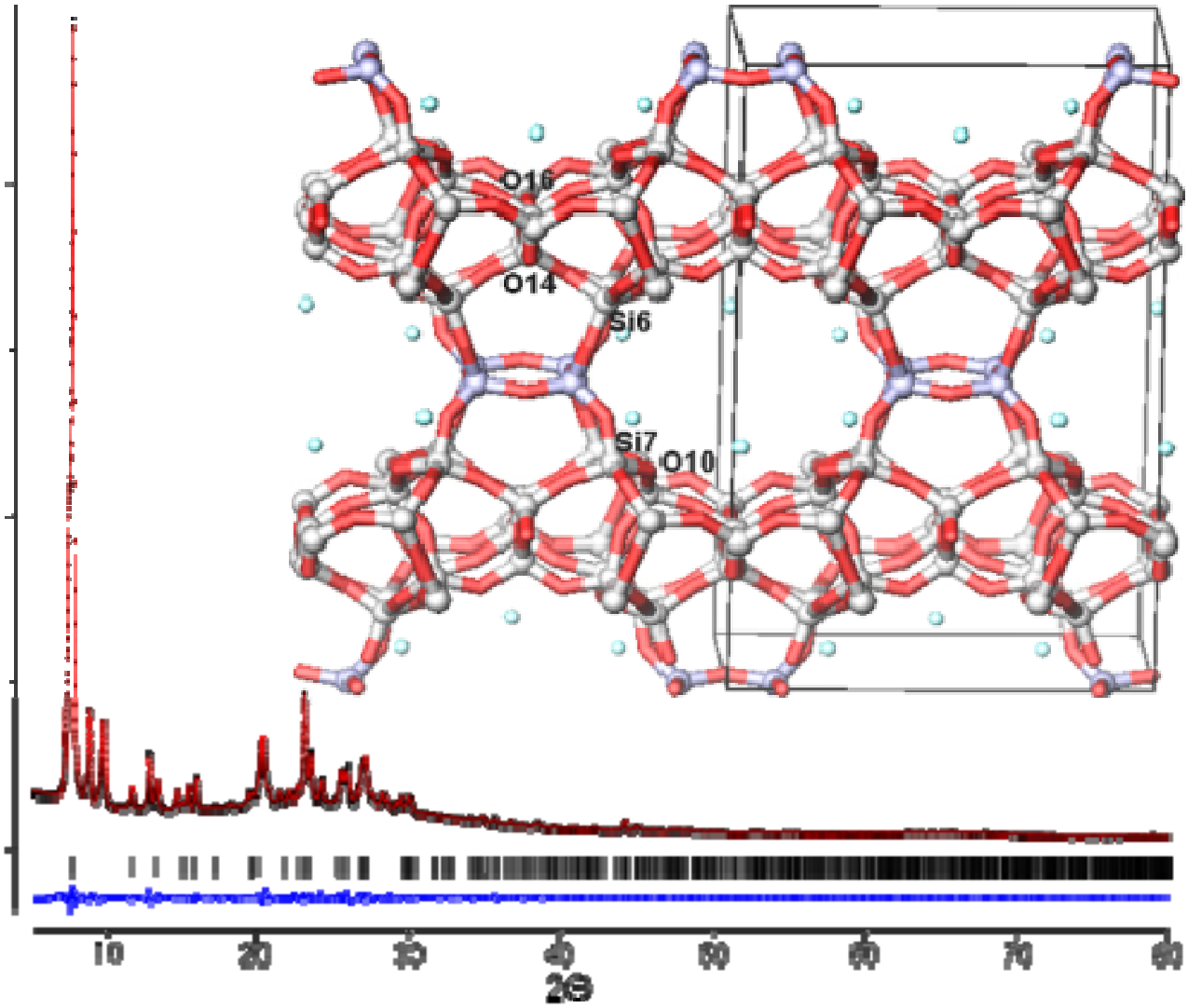

Figure S8 : Rietveld refinement of COK-14 measured on a STOE Stadi MP diffractometer (λ = 1.54056 Å, Rp=2.08%, Rwp=2.9%, RF^2=7.4%). Experimental (black) and calculated (red) XRD patterns as well as the difference profile are shown (blue). The short tick marks below the patterns give the position of the Bragg reflections.

Table S4 : Lattice constants, R-values and bond distances and angles of the refined COK-14.

		***a* (Å)**	***b* (Å)**	***c* (Å)**	***β* (°)**
COK-14	lattice parameters	24.1319 (15)	13.7918(6)	12.2977(4)	109.600(4)

estimated standard deviation in brackets

Radiation	***λ* (Å)**	**R-values (%)**	
$CuK_{\alpha 1}$	1.54056	Rp	2.1
		Rwp	2.9
		RF^2	7.4

Bond	**Distance (Å)**	**Bond**	**Distance (Å)**
Average Si – Si	2.946	Average Si – O	1.613
Minimum Si – Si	2.766	Minimum Si – O	1.546
Maximum Si – Si	3.028	Maximum Si – O	1.622

Bond	**Angle (°)**	**Bond**	**Angle (°)**
Average Si – O – Si	148.614	Average O – Si – O	109.4
Minimum Si – O – Si	117.5	Minimum O – Si – O	102
Maximum Si – O – Si	180	Maximum O – Si – O	125.8

		a (Å)	***b* (Å)**	***c* (Å)**	***β* (°)**
DFT COK-14	lattice parameters	24.47	13.97	12.36	109.38

Bond	**Distance (Å)**	**Bond**	**Distance (Å)**
Si - Si	3.112	Si – O	1.623
Bond	**Angle (°)**	**Bond**	**Angle (°)**
Si – O – Si	151.633	O – Si – O	109.478

DOI: 10.1038/NMAT3455

Structure analysis of -GeCOK-14

The occurrence of a true inverse sigma transformation of UTL type zeolite into COK-14 was further investigated. Attempts were made to capture intermediate states where the layers already were disconnected but the removed fragment not yet washed out. Finally, a sample containing approximately 50% of its original Ge content was obtained by exposing IM-12 to 12 M HCl only for 4 hours at 95 °C.

According to ^{29}Si MAS NMR (Fig. S2) this sample still showed the presence of Si-O-Ge bonds but also revealed presence of Q^3. This led to the first, but wrong assumption this material still has the general structure and large layer distance as the parent material. Surprisingly, the X-ray diffraction pattern clearly showed the layers already were at exactly the same short distance as in the COK-14 framework. This indicated the part removed during the inverse sigma transformation already was dislocated from its original site. Nonetheless, the X-ray diffraction pattern indicated a highly ordered structure. Initial attempts to refine the structure based on starting parameters of COK-14 quickly supported the presence of the siliceous layers at typical distances for –COK-14 and COK-14. Most intriguing was the observation that electron density in the plane of the Si-4R strongly indicated this ring was closed in contrast to the broken structure in the final -COK-14 (Fig. S9, left). Furthermore, significant electron density was observed in the location which was to become the 12-ring channel between the 4Rs in the fully formed structure (Fig. S9). Despite the clear evidence of the layers, the refinement of the layer-connecting 4R and its vicinity failed, because electron density around most atoms in this region appeared not to be sufficiently localised, which led to unreasonable temperature factors. Observation of the electron density therefore revealed significant strain or disorder in the same regions in the intermediate structure as in the fully condensed COK-14 framework. X-ray Absorption Spectroscopy (XAS) spectra recorded at the Ge K-edge were available for the same specimen. The initial basic single scattering analysis of the first coordination shells indicated the presence of oxygen atoms at respectively 1.73 and 1.8 Å. To obtain a basic description of the recorded EXAFS spectra an additional shell containing Ge atoms was necessary. According to the variation of the Debye-Waller factors with the coordination number for this shell and comparison of the fit parameters with a tetrahedral GeO_2 reference, a coordination number of two Ge-neighbours at the distance of 3.2 Å was concluded. Such an arrangement can only be realised in infinite chains or ring-structures. Considering the clustered electron density observed by XRD and the presence of a distinct Ge feature in the real part of the Fourier transformed spectra at r+Δ 4.2 Å, strong indications for the presence of a 4-ring structure were available. Comparison of the EXAFS data with that recorded for a reference UTL sample (1st shell coordination number = 4) readily indicated an average 1st shell coordination number of 4.5 (3.5 at 1.73 Å + 1 at 1.82 Å) assigned to oxygen neighbours. After this initial basic single scattering (SS) analysis, a Ge-4r molecular model was created using one of the 4-rings in the UTL structure as a starting geometry. After adapting the basic 4-ring model geometry to reflect the distances and coordination numbers obtained during the initial basic EXAFS analysis, the theoretical scattering paths for this model were calculated using feff6. The fit results of a more extensive EXAFS analysis using this model, indicated that this provided a fairly accurate description of the experimental EXAFS data, provided that additional O and Si SS paths were included at respectively 2.8, 3.6 and 3.9 Å. To localise the Ge 4-ring indicated from the EXAFS analysis in the Ge-COK-14 structure, the electron density maps obtained from the diffraction data for sample Ge-

COK-14 were revisited (Fig. S9 and Fig. 4 main document). The strong electron density observed between two Si-4R in the 12R channel quickly revealed the presence of a structure which appeared in accordance with the number of neighbours and distances around the Ge centres.

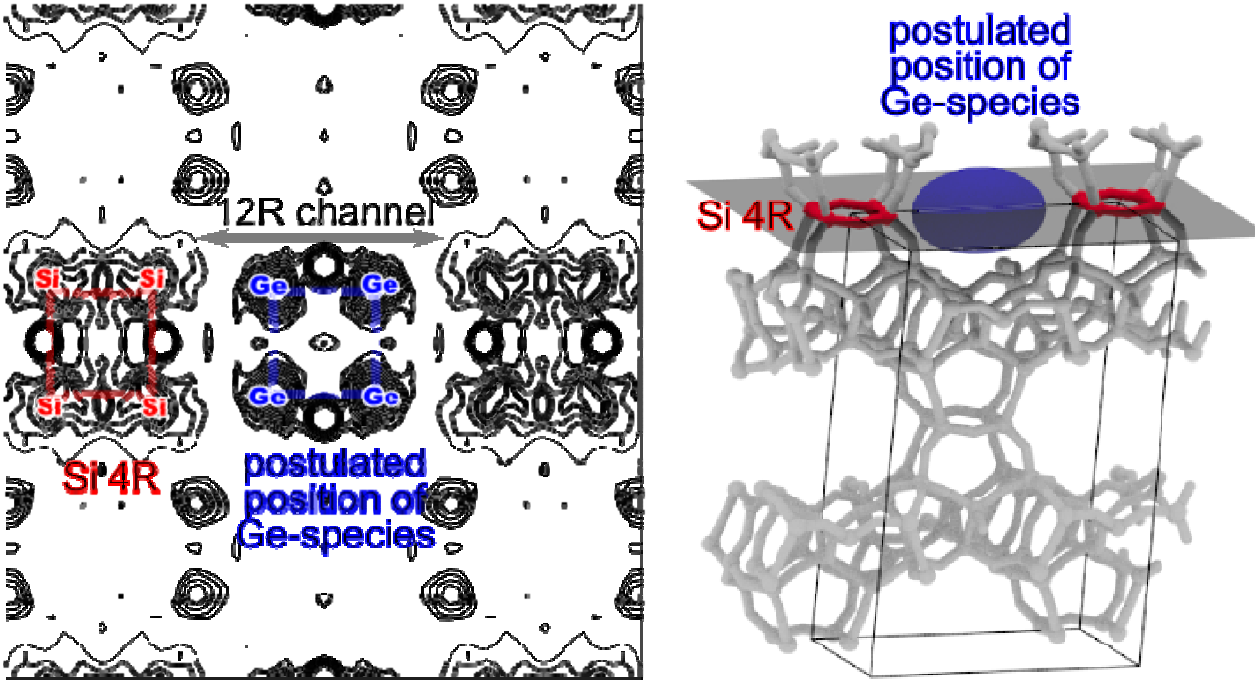

Figure S9 : Left : Electron density in the *bc*-plane centered on 0,1/2,0, cutting through 2 Si-4Rs. Right : Illustration of location of electron density slice projected on the closed COK-14 framework. Si-4Rs are highlighted in red and the region where the germanate species was expected in blue.

Accordingly, a probe species consisting of three atoms, a Ge atom tethered to two oxygen atoms at a distance of 1.74 Å, was inserted in the position observed by electron density analysis and left to refine freely. The oxygen atoms quickly assumed special positions in x,0.5,y and x,y,0, while the Ge atom did not localise in one position without unreasonable temperature factors. Instead, electron density above and below the plane spanned by the oxygen atoms indicated a split position for Ge which was a strong hint the symmetry of the spacegroup C2/m did not correctly describe the structure. As soon as 2 Ge sites were assumed, refinement became stable and R-factors significantly improved. Furthermore, the Ge atoms approached positions in a 4-ring with Ge-Ge and Ge-O distances exactly matching the values obtained in the EXAFS analysis. A similar situation was encountered for the Si atoms of the Si-4R (Si13) and silicon sites (Si6, Si7) connecting to the layers. Consequently, also these sites and the four oxygen sites connecting the Si-4R and layers were split (denoted Si'13, Si'6, Si'7, Oa, Ob, Oc and Od respectively, see Fig. S10 and Table S13). This corresponded to a local doubling of the structure to account for the wrong symmetry in the vicinity of the structural break. Accordingly, the bond and angle constraints in this region also were lifted to allow free drift of the atoms to those sites with highest observed electron density. Like in the case of the Ge-fragment, distances of the doubled Si sites to Ge immediately converged towards values close to EXAFS results (3.6 Å for Si'6-Ge and Si'7-Ge and 3.9 Å for Si'13-Ge). With this set of parameters a search for the positions of the oxygen atoms linked to the germanate and also to Si was

DOI: 10.1038/NMAT3455

performed. The regions surrounding the Ge centres at distances found by EXAFS were systematically analysed for their electron density and oxygen atoms were inserted into the refinement. Initially, the distance of these oxygen atoms to Ge was constrained. It turned out the one long bond between O and Ge of 1.8 Å observed with EXAFS pointed towards the Si atoms at the Si-Ge distance of 3.6 Å, which connected the layer with the Si-4R (Si'6 and Si'7). Final fitted parameters can be found in Table S5.

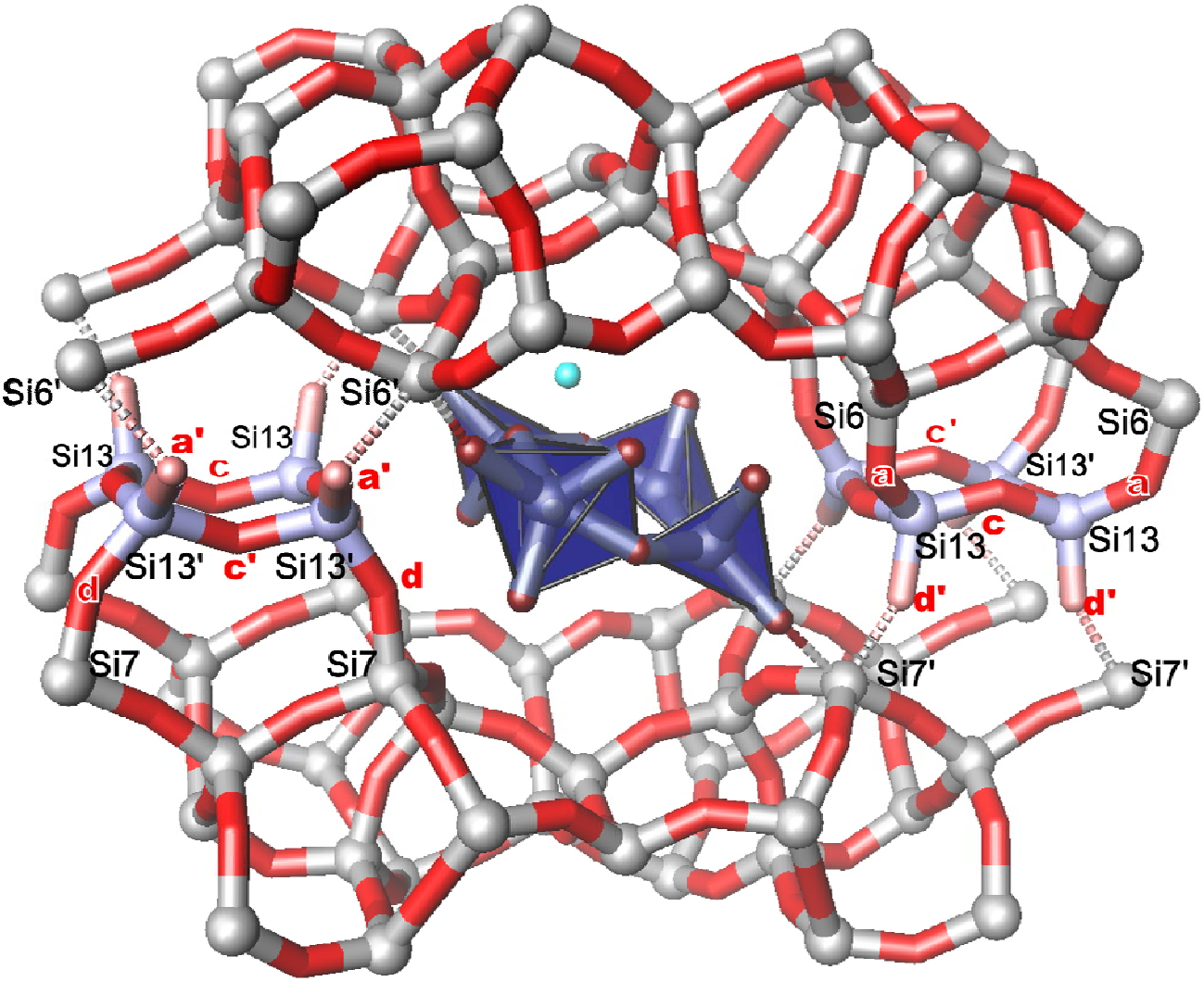

Figure S10 : Detail view of the 4R germanate species located between two Si-4R of the broken layers. The representation is shown in P1. Ge is given in dark blue, Si in 4R in light blue, Si in UTL-type layers in grey. Oxygen associated to Ge are in dark red, associated to silanol in light red. Atom coordinates in P1 representation are listed in table S14.

Eventually, the germanate oligomer was best described as a 4R containing two Ge-centres with 4 direct oxygen neighbours in distorted tetrahedra linked two other Ge-centres in five-fold coordination close to trigonal bipyramidal geometry (Fig. S10). This geometry not only fully corresponded to the coordination observed by EXAFS but is also close to similar structural units encountered in germanates[28,29]. The identified Ge-4R is positioned diagonally in the region of the 12-ring window in the corresponding COK-14 framework and distances

of oxygen atoms associated to Ge to framework atoms Si'6 and Si'7 suggested direct strong interaction of the Ge-4R with both layers. In parallel with construction and refinement of the Ge-fragment the bonding situation of the framework was investigated. From ^{29}Si MAS NMR (Fig. S2) it was known Si occurred in the Ge-COK-14 as Q^3 and as higher coordinated atoms (Q^4) with one or no Ge neighbour. Taking geometry and position of the Ge-species in consideration it was concluded that at least part of the layer connecting Si atoms experienced a 4-fold coordination environment with one Ge neighbour, albeit at a longer distance than in fully connected germano-zeolites. This immediately implies this Si atom (Si'6, Si'7) is not or only weakly linked to the Si-4R, which in turn results in the Si-4R atoms to behave as Q^3 species. Note that in this structure the Si-4R is intact but not linked to both layers contrary to the situation encountered in the interrupted framework of –COK-14. Indeed, there was evidence from the refined coordinates that the Si-4R systematically has lost connection to the neighbouring layer, which instead remained linked to the discovered Ge-fragment. This interpretation would result in the simultaneous presence of a Q^3 and a Q^4-1Ge resonance which is in full agreement with the recorded ^{29}Si-NMR data (Fig. S2). Further support for this model arose from the ^{1}H MAS and wPMLG spectra. The MAS only spectrum, shows a dominant signal at 5.6 ppm and an ensemble around 1.3 ppm. In wPMLG some signals in the 1.3 ppm range disappear, due to weak dipolar couplings. The remaining signal in this range is broader than in MAS only acquisition. This can be assigned to protons associated to silanol and/or germanol. For the signal at 5.6 ppm signals in both MAS and MAS wPMLG are almost identical, indicating a broad coupling between protons as expected for loosely bound water, for example associated to the germanate species or the framework[25]. Surprisingly, even though the space group C2/m cannot reflect the local geometry of the embedded fragment in the broken layers, refinement led to unexpected good description of the experimental pattern with r-values of Rp=4.8%, Rwp=6.5%, RF^2=7.5% (Fig. 4 main document, Fig. S11, Table S6 and S13). Clearly, the parameter set, including the doubled parts of framework and Ge-fragment correctly described the average connectivity in the material. It was analysed if the structure could be described in a different space group but due to the asymmetric structure of Ge-4R and its diagonal arrangement in the channel of the structure the only option turned out to be P1 with a doubling of the *b*-axis. Any choice of a smaller cell would not have accounted for the symmetry of the layers and the Ge-oligomer. The corresponding unit cell contained 485 atoms (Table S14), which clearly ruled out a sensible Rietveld refinement. Furthermore, an inspection of the relation between Ge-species and framework indicated that there may be no direct correlation between the orientations of the Ge-4Rs and that these may be statistically realised. This suggested that even though the C2/m spacegroup does not correctly described the local symmetry, it still should be the best way to describe the material which best is declared as structure following a pseudo-symmetry in C 2/m. Interestingly, the layer distance in this material (d_{100}=11.5 Å) is smaller than in the interrupted framework of -COK-14 (d_{100}=11.6 Å) but still larger than in the fully closed form of COK-14 (d_{100}=11.4 Å). This indicated the remaining 4R of germanium not only has been dislodged but in all probability plays an important role in keeping the disconnected layers at the correct distance and orientation.

DOI: 10.1038/NMAT3455

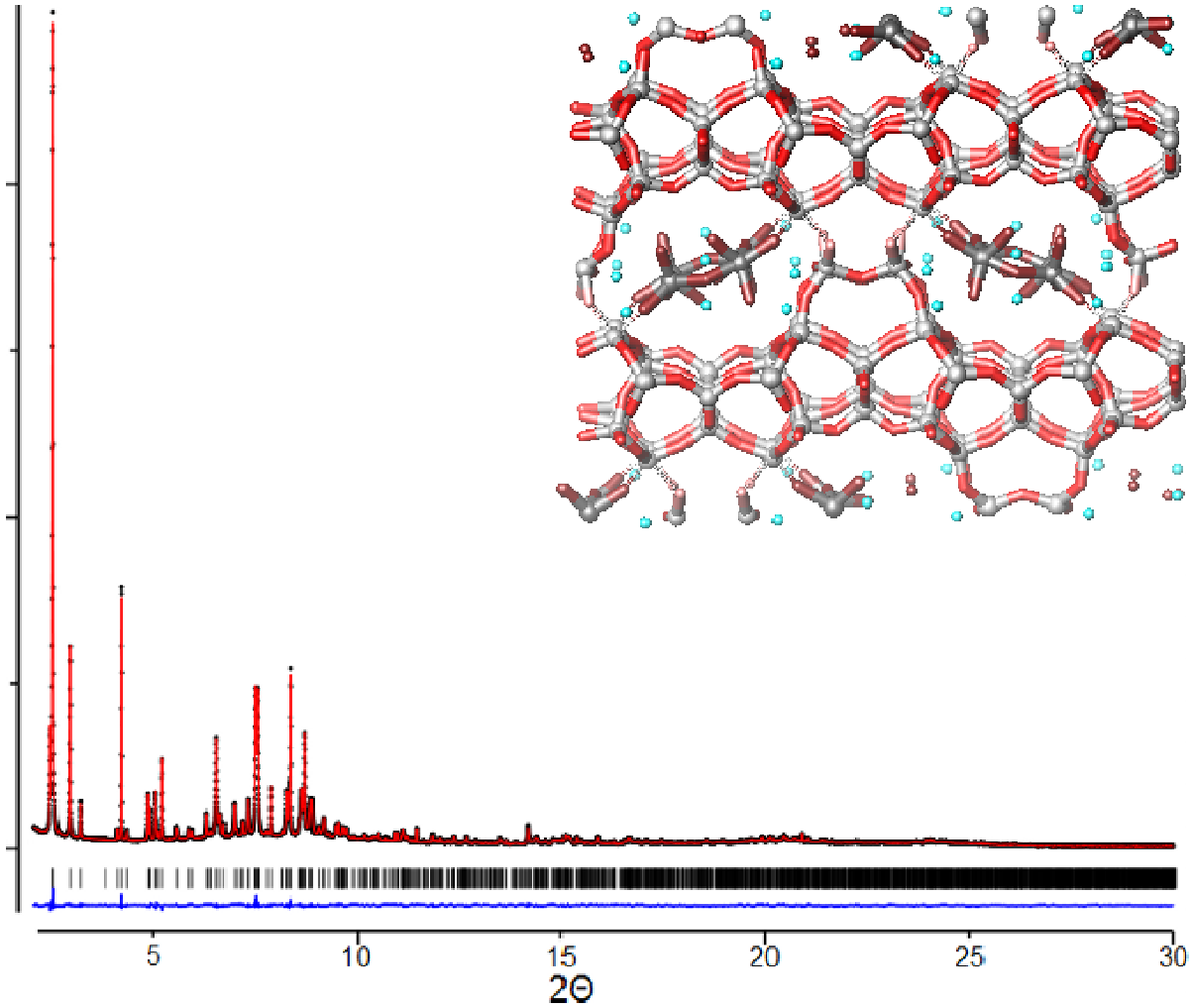

Figure S11 : Expanded part of Fig. 4 main document : Rietveld refinement of Ge-COK-14 measured at the SNBL beamline in Grenoble (λ = 1.1172 Å, Rp=4.8%, Rwp=6.5%, RF^2=7.5%). Experimental (black) and calculated (red) XRD patterns as well as the difference profile are shown (blue). The short tick marks below the pattern give the position of the Bragg reflections. Refinement details can be found in Table S6 and S13.

Table S5 : Fitted EXAFS parameters of Ge-COK-14

Type	N	S_0^2	$sigma^2$	e_0	Δr	R_{model}*	R
O	3.482	1	0.00187	4.963	-0.019	1.746	1.727
O	1	1	0.00187	4.963	-0.012	1.818	1.805
Ge	2	1	0.00587	4.963	-0.017	3.203	3.185
Si	1	1	0.0056	4.963	0.054	3.598	3.652
Si	1	1	0.0056	4.963	-0.101	3.899	3.798
Ge	1	1	0.00673	4.963	0.109	4.427	4.536
O	1.5	1	0.00629	4.963	-0.069	2.831	2.763

*as obtained from Rietveld refinement

Table S6 : Lattice constants, R-values and bond distances and angles of the refined Ge-COK-14. Refinement occurred in C2/m. Bond distances and angles were derived from the structure representation in P1.

	a (Å)	*b (Å)*	*c (Å)*	*β (°)*
lattice parameters	24.43174(26)	13.90230(7)	12.28142(8)	108.9693(21)

estimated standard deviation in brackets

Ge-COK-14

Radiation	***λ (Å)***	**R-values (%)**	
synchrotron	0.502403	Rp	3.9
		Rwp	6.5
		RF^2	7.5
Bond	**Distance (Å)**	**Bond**	**Distance (Å)**
Average Si – Si	3.085	Average Si – O	1.609
Minimum Si – Si	2.96	Minimum Si – O	1.567
Maximum Si – Si	3.18	Maximum Si – O	1.624
Bond	**Angle (°)**	**Bond**	**Angle (°)**
Average Si – O – Si	153.854	Average O – Si – O	109.415
Minimum Si – O – Si	128.427	Minimum O – Si – O	94.993
Maximum Si – O – Si	180	Maximum O – Si – O	129.817
Average Ge – O – Ge	132.623	Average O – Ge – O	107.146
Minimum Ge – O – Ge	132.485	Minimum O – Ge – O	63.578
Maximum Ge – O – Ge	132.76	Maximum O – Ge – O	151.875

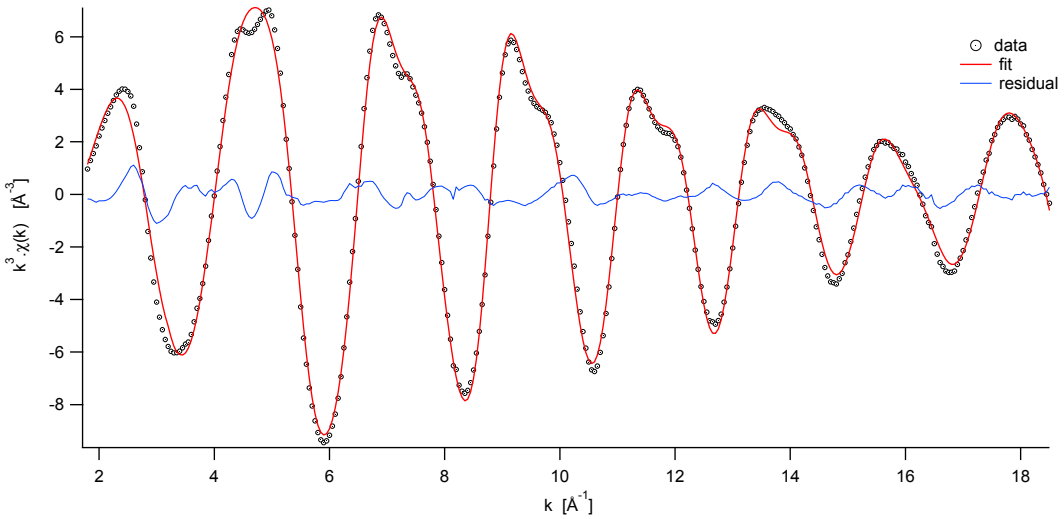

Figure S12 : Expanded part of Fig. 4 main document. k^3 weighted EXAFS spectrum. The final fit of EXAFS data was based on coordinates obtained by Rietveld refinement. Experimental data (black), fitted spectrum (red) and residual (blue) are shown. The fit was performed in k-space, concurrently on k, k^2 and k^3 weighted data. Fitted results are listed in table S5.

DOI: 10.1038/NMAT3455

Arrangement of Ge in the parent UTL structure

To verify a true inverse sigma transformation took place the arrangement of Ge in the parent UTL structure was analysed by EXAFS at the Ge-edge. The EXAFS analysis revealed already in the UTL framework each Ge centre had exactly two Ge neighbours at 3.16 Å and 4 oxygen atoms (3+1) at respectively 1.75 Å and 1.85 Å. All distances are fully compatible with a Ge (4R) already present in the D4R as part of the UTL structure.

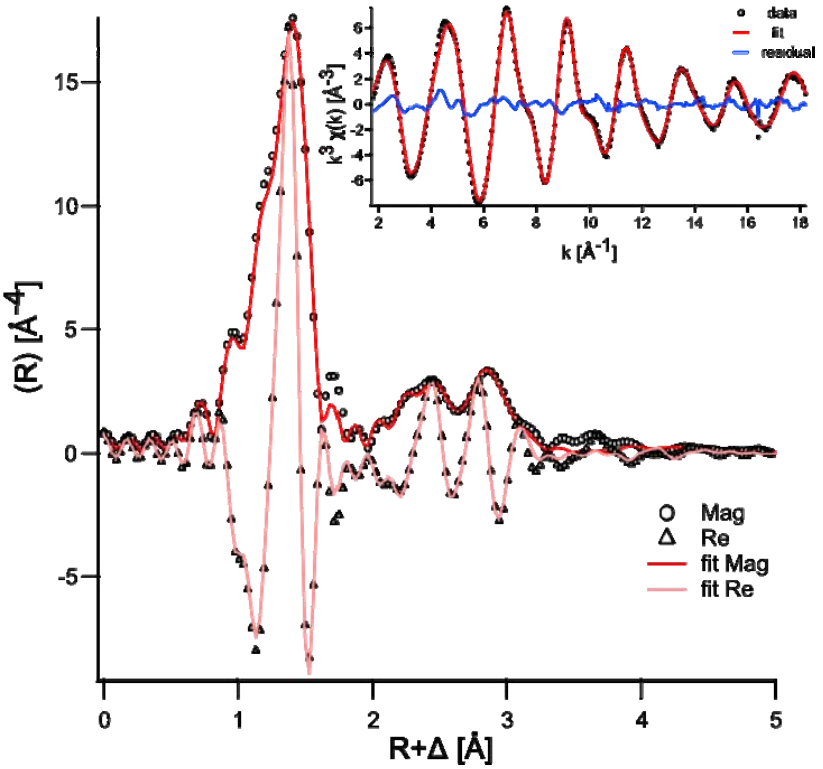

Figure S13 : k^3 weighted EXAFS data as insert and its Fourier transform (magnitude/real part) for IM-12. Fit based on a 4R fragment cut from the UTL topology. Fitted data can be found in Table S7

Table S7 : Fitted EXAFS parameters of IM-12 parent material. Element names refer to UTL structure from literature[30].

Type	N	S_0^2	$sigma^2$	e_0	Δr	R_{model}*	R
O5	3	1	0.00209	7.005	0.032	1.713	1.745
O13	1	1	0.00209	7.005	0.052	1.779	1.831
Ge1	2	1	0.00767	7.005	-0.059	3.212	3.153
Si9	2	1	0.02065	7.005	0.166	3.009	3.175
O2	2	1	0.00502	7.005	-0.023	2.823	2.8
Ge2	1	1	0.01234	7.005	-0.075	4.524	4.449

*as obtained from UTL topology

Listing of atomic coordinates as obtained from Rietveld refinement and DFT simulation

-COK-14

Rietveld, synchrotron

Table S8: Atomic coordinates of hydrated -COK-14 equilibrated with ambient humidity using synchrotron radiation (λ = 1.1172 Å). The number between brackets gives the esd. -COK-14 has a unit cell of *a* = 24.6355 (10) Å. *b* = 13.93666 (23) Å. *c* = 12.2637 (4) Å and a monoclinic angle of 109.2189 (33°) ° with a space group C 2/m. Bond angle and distance restraints in final refinement were weighted by a factor of 0.2 (Rp=2.60 %, Rwp=3.31 %, RF^2=8.77 %).

T atom name	x coordinate	y coordinate	z coordinate	Uiso	Site Multiplicity
Si3	0.30471(29)	0.7933(6)	0.2420(7)	0.053(4)	8
Si4	0.30985(23)	0.7954(4)	0.5041(5)	0.0374(35)	8
Si5	0.31752(22)	0.7967(4)	0.8754(5)	0.0056(22)	8
Si6	0.37476(22)	0.7027(4)	0.1151(5)	0.072(5)	8
Si7	0.38272(22)	0.7008(4)	0.7247(5)	0.0311(32)	8
Si8	0.27426(25)	0	0.7981(5)	0.045(7)	4
Si9	0.23313(25)	0.5	0.8271(5)	0.0222(23)	4
Si10	0.32465(25)	0.5	0.6924(5)	0.029(5)	4
Si11	0.22927(25)	0.5	0.4629(5)	0.064(8)	4
Si12	0.31454(25)	0.5	0.0834(5)	0.010(4)	4
Si13	0.99739(19)	0.74833(26)	0.12502(9)	0.030(5)	8
O1	0.30638(32)	0.90637(30)	0.2155(9)	0.036(9)	8
O2	0.35930(29)	0.7410(7)	0.2249(5)	0.094(24)	8
O3	0.3121(4)	0.7795(8)	0.3755(4)	0.072(10)	8
O4	0.24642(22)	0.7451(6)	0.1642(9)	0.009(6)	8
O5	0.30839(28)	0.90753(27)	0.5284(8)	0.018(4)	8
O6	0.25	0.75	0.5	0.127(12)	4
O7	0.36177(30)	0.7401(6)	0.5941(5)	0.011(6)	8
O8	0.3459(4)	0.7723(6)	0.0090(4)	0.012(7)	8
O9	0.31215(34)	0.90980(28)	0.8604(8)	0.062(10)	8
O10	0.35478(23)	0.7612(6)	0.8014(4)	0.122(15)	8
O11	0.35323(28)	0.59386(28)	0.0869(10)	0.070(30)	8
O13	0.36626(28)	0.59136(27)	0.7271(9)	0.013(5)	8
O14	0.21131(23)	0	0.8115(5)	0.097(19)	4
O15	0.2654(4)	0	0.6635(4)	0.056(14)	4
O16	0.2616(4)	0.5	0.9640(4)	0.036(6)	4

DOI: 10.1038/NMAT3455

O17	0.28149(22)	0.5	0.7654(5)	0.056(17)	4
O18	0.29281(32)	0.5	0.5558(5)	0.057(5)	4
O19	0.04878(24)	0.7937(7)	0.2212(8)	0.005(6)	8
O31	0.9995(9)	0.6300(7)	0.1329(15)	0.080(5)	8
O21	0.94267(22)	0.7934(8)	0.1413(9)	0.093(11)	8
O22	0	0.7759(11)	0	0.027(12)	4

Rietveld, CuK$_{\alpha 1}$

Table S9: Atomic coordinates of the partially dried -COK-14 structure measured on a STOE Stadi MP diffractometer (λ = 1.54056 Å). The number between brackets gives the esd. -COK-14 has a unit cell of *a* = 24.6406 (6) Å. *b* = 13.92386 (21) Å. *c* = 12.25976 (28) Å and a monoclinic angle of 109.1961 (21)° with a space group C 2/m. Bond angle and distance restraints in final refinement were weighted by a factor of 0.2 (Rp=3.20 %, Rwp=4.50 %, RF^2=11.35 %).

T atom	x	y	z	Uiso	Site
Si3	0.31021(15)	0.79846(33)	0.2497(4)	0.081(4)	8
Si4	0.31060(12)	0.79805(22)	0.51027(25)	0.0258(30)	8
Si5	0.31417(12)	0.79339(21)	0.87689(25)	0.0214(26)	8
Si6	0.37463(12)	0.70467(21)	0.11697(24)	0.0188(20)	8
Si7	0.38344(12)	0.69916(22)	0.73242(25)	0.0481(33)	8
Si8	0.26950(13)	0	0.81417(26)	0.026(5)	4
Si9	0.22687(13)	0.5	0.81611(27)	0.055(5)	4
Si10	0.31709(13)	0.5	0.68213(26)	0.027(5)	4
Si11	0.23118(12)	0.5	0.44552(27)	0.040(5)	4
Si12	0.32245(13)	0.5	0.06868(26)	0.007(4)	4
Si13	1.00219(13)	0.7514(4)	0.12116(25)	0.05708	8
O1	0.31345(15)	0.90554(15)	0.2055(5)	0.057(8)	8
O2	0.35776(15)	0.7296(4)	0.22965(25)	0.085(9)	8
O3	0.32109(19)	0.7969(5)	0.38768(21)	0.074(8)	8
O4	0.24672(11)	0.75589(32)	0.1877(5)	0.168(7)	8
O5	0.30773(14)	0.90776(14)	0.5493(4)	0.092(10)	8
O6	0.25	0.75	0.5	0.071(19)	4
O7	0.36245(15)	0.74407(29)	0.60486(24)	0.066(4)	8
O8	0.33362(21)	0.76705(31)	0.01179(22)	0.059(8)	8
O9	0.30773(17)	0.90786(14)	0.8701(5)	0.025(6)	8
O10	0.36273(12)	0.76251(31)	0.82170(24)	0.091(10)	8
O11	0.36263(14)	0.59353(14)	0.0825(5)	0.017(7)	8
O13	0.35586(15)	0.59378(14)	0.7287(5)	0.018(7)	8
O14	0.20769(11)	0	0.83278(25)	0.013(9)	4
O15	0.25819(21)	0	0.67732(19)	0.097(11)	4
O16	0.27289(20)	0.5	0.94465(24)	0.050(6)	4
O17	0.26232(11)	0.5	0.72643(24)	0.085(18)	4
O18	0.29377(17)	0.5	0.54300(25)	0.094(12)	4
O19	0.04776(12)	0.81065(34)	0.2250(4)	0.106(11)	8
O31	1.0192(4)	0.6426(4)	0.1267(8)	0.010(7)	8
O21	0.94035(9)	0.7663(4)	0.1382(4)	0.022(4)	8
O22	0	0.8005(5)	0	0.0229(4)	4

DOI: 10.1038/NMAT3455

DFT

Table S10: Atomic coordinates of -COK-14 calculated by DFT. The calculations start from the experimentally proposed crystal structure without specifying any symmetry group. The output shows a structure that deviates only very slightly from the experimental C2/m space group (a = 25.1 Å. b = 14.2 Å c = 12.5 Å. β = 109°) but is strictly spoken of P1 symmetry. The strong coincidence of the parameters obtained in P1 with sites in C2/m indicates the latter most probably to be the true space-group of the material. Coordinates of all atoms simulated in P1 are given below.

T atom	x coordinate	y coordinate	z coordinate	T atom	x coordinate	y coordinate	z coordinate
Si1	0.30813	0.79701	0.24697	O37	0.81102	0.4075	0.53788
Si2	0.69187	0.20299	0.75303	O38	0.18898	0.5925	0.46212
Si3	0.69187	0.79701	0.75303	O39	0.18898	0.4075	0.46212
Si4	0.30813	0.20299	0.24697	O40	0.81102	0.5925	0.53788
Si5	0.80813	0.29701	0.24697	O41	0.25	0.75	0.5
Si6	0.19187	0.70299	0.75303	O42	0.75	0.25	0.5
Si7	0.19187	0.29701	0.75303	O43	0.75	0.75	0.5
Si8	0.80813	0.70299	0.24697	O44	0.25	0.25	0.5
Si9	0.30963	0.79682	0.50354	O45	0.36211	0.74302	0.59482
Si10	0.69037	0.20318	0.49646	O46	0.63789	0.25698	0.40518
Si11	0.69037	0.79682	0.49646	O47	0.63789	0.74302	0.40518
Si12	0.30963	0.20318	0.50354	O48	0.36211	0.25698	0.59482
Si13	0.80963	0.29682	0.50354	O49	0.86211	0.24302	0.59482
Si14	0.19037	0.70318	0.49646	O50	0.13789	0.75698	0.40518
Si15	0.19037	0.29682	0.49646	O51	0.13789	0.24302	0.40518
Si16	0.80963	0.70318	0.50354	O52	0.86211	0.75698	0.59482
Si17	0.3144	0.79511	0.87298	O53	0.34435	0.76743	0.00469
Si18	0.6856	0.20489	0.12702	O54	0.65565	0.23257	0.99531
Si19	0.6856	0.79511	0.12702	O55	0.65565	0.76743	0.99531
Si20	0.3144	0.20489	0.87298	O56	0.34435	0.23257	0.00469
Si21	0.8144	0.29511	0.87298	O57	0.84435	0.26743	0.00469
Si22	0.1856	0.70489	0.12702	O58	0.15565	0.73257	0.99531
Si23	0.1856	0.29511	0.12702	O59	0.15565	0.26743	0.99531
Si24	0.8144	0.70489	0.87298	O60	0.84435	0.73257	0.00469
Si25	0.37416	0.69957	0.11263	O61	0.31	0.90872	0.86476
Si26	0.62584	0.30043	0.88737	O62	0.69	0.09128	0.13524
Si27	0.62584	0.69957	0.88737	O63	0.69	0.90872	0.13524
Si28	0.37416	0.30043	0.11263	O64	0.31	0.09128	0.86476
Si29	0.87416	0.19957	0.11263	O65	0.81	0.40872	0.86476
Si30	0.12584	0.80043	0.88737	O66	0.19	0.59128	0.13524

Si31	0.12584	0.19957	0.88737	O67	0.19	0.40872	0.13524
Si32	0.87416	0.80043	0.11263	O68	0.81	0.59128	0.86476
Si33	0.3812	0.6994	0.72242	O69	0.3526	0.761	0.79841
Si34	0.6188	0.3006	0.27758	O70	0.6474	0.239	0.20159
Si35	0.6188	0.6994	0.27758	O71	0.6474	0.761	0.20159
Si36	0.3812	0.3006	0.72242	O72	0.3526	0.239	0.79841
Si37	0.8812	0.1994	0.72242	O73	0.8526	0.261	0.79841
Si38	0.1188	0.8006	0.27758	O74	0.1474	0.739	0.20159
Si39	0.1188	0.1994	0.27758	O75	0.1474	0.261	0.20159
Si40	0.8812	0.8006	0.72242	O76	0.8526	0.739	0.79841
Si41	0.27397	0	0.8038	O77	0.35196	0.59252	0.08457
Si42	0.72603	0	0.1962	O78	0.64804	0.40748	0.91543
Si43	0.77397	0.5	0.8038	O79	0.64804	0.59252	0.91543
Si44	0.22603	0.5	0.1962	O80	0.35196	0.40748	0.08457
Si45	0.23058	0.5	0.82158	O81	0.85196	0.09252	0.08457
Si46	0.76942	0.5	0.17842	O82	0.14804	0.90748	0.91543
Si47	0.73058	0	0.82158	O83	0.14804	0.09252	0.91543
Si48	0.26942	0	0.17842	O84	0.85196	0.90748	0.08457
Si49	0.32098	0.5	0.68617	O85	0.36083	0.59141	0.71865
Si50	0.67902	0.5	0.31383	O86	0.63917	0.40859	0.28135
Si51	0.82098	0	0.68617	O87	0.63917	0.59141	0.28135
Si52	0.17902	0	0.31383	O88	0.36083	0.40859	0.71865
Si53	0.22499	0.5	0.45168	O89	0.86083	0.09141	0.71865
Si54	0.77501	0.5	0.54832	O90	0.13917	0.90859	0.28135
Si55	0.72499	0	0.45168	O91	0.13917	0.09141	0.28135
Si56	0.27501	0	0.54832	O92	0.86083	0.90859	0.71865
Si57	0.31363	0.5	0.07703	O93	0.21196	0	0.81868
Si58	0.68637	0.5	0.92297	O94	0.78804	0	0.18132
Si59	0.81363	0	0.07703	O95	0.71196	0.5	0.81868
Si60	0.18637	0	0.92297	O96	0.28804	0.5	0.18132
Si61	0.99701	0.75447	0.12432	O97	0.26387	0	0.66881
Si62	0.00299	0.24553	0.87568	O98	0.73613	0	0.33119
Si63	0.00299	0.75447	0.87568	O99	0.76387	0.5	0.66881
Si64	0.99701	0.24553	0.12432	O100	0.23613	0.5	0.33119
Si65	0.49701	0.25447	0.12432	O101	0.2615	0.5	0.9579
Si66	0.50299	0.74553	0.87568	O102	0.7385	0.5	0.0421
Si67	0.50299	0.25447	0.87568	O103	0.7615	0	0.9579

DOI: 10.1038/NMAT3455

Si68	0.49701	0.74553	0.12432	O104	0.2385	0	0.0421
O1	0.30954	0.90777	0.21493	O105	0.27753	0.5	0.75787
O2	0.69046	0.09223	0.78507	O106	0.72247	0.5	0.24213
O3	0.69046	0.90777	0.78507	O107	0.77753	0	0.75787
O4	0.30954	0.09223	0.21493	O108	0.22247	0	0.24213
O5	0.80954	0.40777	0.21493	O109	0.28622	0.5	0.55082
O6	0.19046	0.59223	0.78507	O110	0.71378	0.5	0.44918
O7	0.19046	0.40777	0.78507	O111	0.78622	0	0.55082
O8	0.80954	0.59223	0.21493	O112	0.21378	0	0.44918
O9	0.35881	0.74117	0.22065	O113	0.05097	0.79835	0.22281
O10	0.64119	0.25883	0.77935	O114	0.94903	0.20165	0.77719
O11	0.64119	0.74117	0.77935	O115	0.94903	0.79835	0.77719
O12	0.35881	0.25883	0.22065	O116	0.05097	0.20165	0.22281
O13	0.85881	0.24117	0.22065	O117	0.55097	0.29835	0.22281
O14	0.14119	0.75883	0.77935	O118	0.44903	0.70165	0.77719
O15	0.14119	0.24117	0.77935	O119	0.44903	0.29835	0.77719
O16	0.85881	0.75883	0.22065	O120	0.55097	0.70165	0.22281
O17	0.31733	0.78601	0.38073	O121	0.99517	0.64328	0.13821
O18	0.68267	0.21399	0.61927	O122	0.00483	0.35672	0.86179
O19	0.68267	0.78601	0.61927	O123	0.00483	0.64328	0.86179
O20	0.31733	0.21399	0.38073	O124	0.99517	0.35672	0.13821
O21	0.81733	0.28601	0.38073	O125	0.49517	0.14328	0.13821
O22	0.18267	0.71399	0.61927	O126	0.50483	0.85672	0.86179
O23	0.18267	0.28601	0.61927	O127	0.50483	0.14328	0.86179
O24	0.81733	0.71399	0.38073	O128	0.49517	0.85672	0.13821
O25	0.24773	0.75227	0.17238	O129	0.94172	0.80224	0.14158
O26	0.75227	0.24773	0.82762	O130	0.05828	0.19776	0.85842
O27	0.75227	0.75227	0.82762	O131	0.05828	0.80224	0.85842
O28	0.24773	0.24773	0.17238	O132	0.94172	0.19776	0.14158
O29	0.74773	0.25227	0.17238	O133	0.44172	0.30224	0.14158
O30	0.25227	0.74773	0.82762	O134	0.55828	0.69776	0.85842
O31	0.25227	0.25227	0.82762	O135	0.55828	0.30224	0.85842
O32	0.74773	0.74773	0.17238	O136	0.44172	0.69776	0.14158
O33	0.31102	0.9075	0.53788	O137	0	0.78271	0
O34	0.68898	0.0925	0.46212	O138	0	0.21729	0
O35	0.68898	0.9075	0.46212	O139	0.5	0.28271	0
O36	0.31102	0.0925	0.53788	O140	0.5	0.71729	0

COK-14

Rietveld, CuK$_{\alpha 1}$

Table S11: Atomic coordinates of the fully condensed COK-14 structure measured on a STOE Stadi MP diffractometer (λ = 1.54056 Å). The number between brackets gives the esd. COK-14 has a unit cell of *a* = 24.1319 (15) Å, *b* = 13.7918 (6) Å, *c* = 12.2977 (4) Å and a monoclinic angle of 109.600 (4)° with a space group C 2/m. Bond angle and distance restraints in final refinement were weighted by a factor of 0.8 (Rp=2.08 %, Rwp=2.89 %, RF^2=7.42 %).

T atom	x	y	z	Uiso	Site
Si3	0.3016(4)	0.7914(6)	0.2446(8)	0.010(7)	8
Si4	0.31311(23)	0.7914(5)	0.5034(8)	0.093(12)	8
Si5	0.32518(35)	0.7955(5)	0.8730(8)	0.027(9)	8
Si6	0.3707(4)	0.6846(7)	0.1016(9)	0.047(9)	8
Si7	0.3840(4)	0.7052(6)	0.7340(9)	0.026(8)	8
Si8	0.2694(6)	0.0	0.8014(11)	0.066(15)	4
Si9	0.2208(6)	0.5	0.8210(13)	0.028(11)	4
Si10	0.3187(5)	0.5	0.6964(10)	0.005(8)	4
Si11	0.2222(6)	0.5	0.4547(11)	0.004(12)	4
Si12	0.2990(7)	0.5	0.0577(14)	0.036(31)	4
Si13	0.0003(6)	0.8868(7)	0.1250(12)	0.081(10)	8
O1	0.3174(6)	0.9033(5)	0.2284(14)	0.042(25)	8
O2	0.3399(7)	0.7215(9)	0.1924(11)	0.090(9)	8
O3	0.3216(7)	0.7695(10)	0.3811(8)	0.032(10)	8
O4	0.2319(5)	0.7702(11)	0.1901(14)	0.038(16)	8
O5	0.3147(6)	0.9064(5)	0.5290(16)	0.088(18)	8
O6	0.25	0.75	0.5	0.061(15)	4
O7	0.3651(5)	0.7327(11)	0.5984(9)	0.019(17)	8
O8	0.3616(8)	0.7687(10)	0.0054(9)	0.058(31)	8
O9	0.3052(6)	0.9075(5)	0.8716(12)	0.069(10)	8
O10	0.36954	0.79307	0.79993	0.127(24)	8
O11	0.3333(7)	0.5933(6)	0.0319(13)	0.053(25)	8
O13	0.3577(6)	0.5974(5)	0.7352(14)	0.046(29)	8
O14	0.2047(7)	0.0	0.8134(15)	0.09(9)	4
O15	0.2667(8)	0.0	0.6680(12)	0.078(14)	4
O16	0.2347(8)	0.5	0.9591(12)	0.081(23)	4
O17	0.2756(9)	0.5	0.7732(20)	0.009(4)	4
O18	0.2850(8)	0.5	0.5584(11)	0.051(15)	4
O19	0.0456(5)	0.8136(10)	0.2152(16)	0.013(14)	8
Oa	0.9377(4)	0.8535(13)	0.1340(18)	0.005(12)	8
Ob	0.0	0.127(4)	0.0	0.089(13)	4
Oc	0.0103(13)	0.0	0.1618(34)	0.028(4)	4
O36	-0.0303(31)	-0.246(4)	0.594(5)	0.025	8
O41	-0.075(4)	0.5	0.583(8)	0.025	4

DOI: 10.1038/NMAT3455

DFT

Table S12 : Atomic coordinates of COK-14 calculated by DFT. The calculations start from the experimentally proposed crystal structure without specifying any symmetry group. The output shows a structure that deviates only very slightly from the experimental C2/m space group (a = 24.4710 Å. b = 13.9669 Å c = 12.3646 Å. β = 109.3832°) but is strictly spoken of P1 symmetry.

T atom	x coordinate	y coordinate	z coordinate	T atom	x coordinate	y coordinate	z coordinate
Si1	0.30993	0.79287	0.24553	O35	0.68167	0.90453	0.45489
Si2	0.69007	0.20713	0.75447	O36	0.31833	0.09547	0.54511
Si3	0.69007	0.79287	0.75447	O37	0.81833	0.40453	0.54511
Si4	0.30993	0.20713	0.24553	O38	0.18167	0.59547	0.45489
Si5	0.80993	0.29287	0.24553	O39	0.18167	0.40453	0.45489
Si6	0.19007	0.70713	0.75447	O40	0.81833	0.59547	0.54511
Si7	0.19007	0.29287	0.75447	O41	0.25	0.75	0.5
Si8	0.80993	0.70713	0.24553	O42	0.75	0.25	0.5
Si9	0.31284	0.79214	0.50562	O43	0.75	0.75	0.5
Si10	0.68716	0.20786	0.49438	O44	0.25	0.25	0.5
Si11	0.68716	0.79214	0.49438	O45	0.36462	0.73021	0.59543
Si12	0.31284	0.20786	0.50562	O46	0.63538	0.26979	0.40457
Si13	0.81284	0.29214	0.50562	O47	0.63538	0.73021	0.40457
Si14	0.18716	0.70786	0.49438	O48	0.36462	0.26979	0.59543
Si15	0.18716	0.29214	0.49438	O49	0.86462	0.23021	0.59543
Si16	0.81284	0.70786	0.50562	O50	0.13538	0.76979	0.40457
Si17	0.31773	0.79378	0.87327	O51	0.13538	0.23021	0.40457
Si18	0.68227	0.20622	0.12673	O52	0.86462	0.76979	0.59543
Si19	0.68227	0.79378	0.12673	O53	0.35226	0.7743	0.00819
Si20	0.31773	0.20622	0.87327	O54	0.64774	0.2257	0.99181
Si21	0.81773	0.29378	0.87327	O55	0.64774	0.7743	0.99181
Si22	0.18227	0.70622	0.12673	O56	0.35226	0.2257	0.00819
Si23	0.18227	0.29378	0.12673	O57	0.85226	0.2743	0.00819
Si24	0.81773	0.70622	0.87327	O58	0.14774	0.7257	0.99181
Si25	0.37108	0.68855	0.10198	O59	0.14774	0.2743	0.99181
Si26	0.62892	0.31145	0.89802	O60	0.85226	0.7257	0.00819
Si27	0.62892	0.68855	0.89802	O61	0.30493	0.90692	0.85981
Si28	0.37108	0.31145	0.10198	O62	0.69507	0.09308	0.14019
Si29	0.87108	0.18855	0.10198	O63	0.69507	0.90692	0.14019
Si30	0.12892	0.81145	0.89802	O64	0.30493	0.09308	0.85981
Si31	0.12892	0.18855	0.89802	O65	0.80493	0.40692	0.85981
Si32	0.87108	0.81145	0.10198	O66	0.19507	0.59308	0.14019
Si33	0.38144	0.69197	0.72684	O67	0.19507	0.40692	0.14019
Si34	0.61856	0.30803	0.27316	O68	0.80493	0.59308	0.85981
Si35	0.61856	0.69197	0.27316	O69	0.36051	0.77133	0.80037

Si36	0.38144	0.30803	0.72684	O70	0.63949	0.22867	0.19963
Si37	0.88144	0.19197	0.72684	O71	0.63949	0.77133	0.19963
Si38	0.11856	0.80803	0.27316	O72	0.36051	0.22867	0.80037
Si39	0.11856	0.19197	0.27316	O73	0.86051	0.27133	0.80037
Si40	0.88144	0.80803	0.72684	O74	0.13949	0.72867	0.19963
Si41	0.26959	1	0.79713	O75	0.13949	0.27133	0.19963
Si42	0.73041	1	0.20287	O76	0.86051	0.72867	0.80037
Si43	0.76959	0.5	0.79713	O77	0.33619	0.59362	0.04096
Si44	0.23041	0.5	0.20287	O78	0.66381	0.40638	0.95904
Si45	0.21122	0.5	0.81911	O79	0.66381	0.59362	0.95904
Si46	0.78878	0.5	0.18089	O80	0.33619	0.40638	0.04096
Si47	0.71122	0	0.81911	O81	0.83619	0.09362	0.04096
Si48	0.28878	0	0.18089	O82	0.16381	0.90638	0.95904
Si49	0.30911	0.5	0.69696	O83	0.16381	0.09362	0.95904
Si50	0.69089	0.5	0.30304	O84	0.83619	0.90638	0.04096
Si51	0.80911	1	0.69696	O85	0.34906	0.59324	0.73605
Si52	0.19089	1	0.30304	O86	0.65094	0.40676	0.26395
Si53	0.21935	0.5	0.45092	O87	0.65094	0.59324	0.26395
Si54	0.78065	0.5	0.54908	O88	0.34906	0.40676	0.73605
Si55	0.71935	0	0.45092	O89	0.84906	0.09324	0.73605
Si56	0.28065	0	0.54908	O90	0.15094	0.90676	0.26395
Si57	0.30116	0.5	0.05742	O91	0.15094	0.09324	0.26395
Si58	0.69884	0.5	0.94258	O92	0.84906	0.90676	0.73605
Si59	0.80116	1	0.05742	O93	0.20648	0	0.81608
Si60	0.19884	1	0.94258	O94	0.79352	0	0.18392
Si61	0.99706	0.88579	0.12873	O95	0.70648	0.5	0.81608
Si62	0.00294	0.11421	0.87127	O96	0.29352	0.5	0.18392
Si63	0.00294	0.88579	0.87127	O97	0.26074	0	0.66167
Si64	0.99706	0.11421	0.12873	O98	0.73926	0	0.33833
Si65	0.49706	0.38579	0.12873	O99	0.76074	0.5	0.66167
Si66	0.50294	0.61421	0.87127	O100	0.23926	0.5	0.33833
Si67	0.50294	0.38579	0.87127	O101	0.23808	0.5	0.95804
Si68	0.49706	0.61421	0.12873	O102	0.76192	0.5	0.04196
O1	0.32648	0.90243	0.22095	O103	0.73808	0	0.95804
O2	0.67352	0.09757	0.77905	O104	0.26192	0	0.04196
O3	0.67352	0.90243	0.77905	O105	0.2616	0.5	0.76094
O4	0.32648	0.09757	0.22095	O106	0.7384	0.5	0.23906
O5	0.82648	0.40243	0.22095	O107	0.7616	0	0.76094
O6	0.17352	0.59757	0.77905	O108	0.2384	0	0.23906
O7	0.17352	0.40243	0.77905	O109	0.27922	0.5	0.55897
O8	0.82648	0.59757	0.22095	O110	0.72078	0.5	0.44103
O9	0.35401	0.71951	0.21366	O111	0.77922	0	0.55897
O10	0.64599	0.28049	0.78634	O112	0.22078	0	0.44103

DOI: 10.1038/NMAT3455

O11	0.64599	0.71951	0.78634	O113	0.04969	0.82784	0.22097
O12	0.35401	0.28049	0.21366	O114	0.95031	0.17216	0.77903
O13	0.85401	0.21951	0.21366	O115	0.95031	0.82784	0.77903
O14	0.14599	0.78049	0.78634	O116	0.04969	0.17216	0.22097
O15	0.14599	0.21951	0.78634	O117	0.54969	0.32784	0.22097
O16	0.85401	0.78049	0.21366	O118	0.45031	0.67216	0.77903
O17	0.3195	0.78091	0.38063	O119	0.45031	0.32784	0.77903
O18	0.6805	0.21909	0.61937	O120	0.54969	0.67216	0.22097
O19	0.6805	0.78091	0.61937	O121	0.99907	1	0.15939
O20	0.3195	0.21909	0.38063	O122	0.00093	1	0.84061
O21	0.8195	0.28091	0.38063	O123	0.50093	0.5	0.84061
O22	0.1805	0.71909	0.61937	O124	0.49907	0.5	0.15939
O23	0.1805	0.28091	0.61937	O125	0.93936	0.83562	0.13952
O24	0.8195	0.71909	0.38063	O126	0.06064	0.16438	0.86048
O25	0.24235	0.76861	0.1705	O127	0.06064	0.83562	0.86048
O26	0.75765	0.23139	0.8295	O128	0.93936	0.16438	0.13952
O27	0.75765	0.76861	0.8295	O129	0.43936	0.33562	0.13952
O28	0.24235	0.23139	0.1705	O130	0.56064	0.66438	0.86048
O29	0.74235	0.26861	0.1705	O131	0.56064	0.33562	0.86048
O30	0.25765	0.73139	0.8295	O132	0.43936	0.66438	0.13952
O31	0.25765	0.26861	0.8295	O133	1	0.87251	1
O32	0.74235	0.73139	0.1705	O134	1	0.12749	1
O33	0.31833	0.90453	0.54511	O135	0.5	0.37251	1
O34	0.68167	0.09547	0.45489	O136	0.5	0.62749	1

Ge-COK-14

Rietveld, CuK$_{\alpha 1}$

Table S13: Atomic coordinates of the Ge-COK-14 structure measured on a SNBL diffractometer (λ = 0.502403 Å) with a spacegroup C 2/m. The number between brackets gives the esd. Ge-COK-14 has a unit cell of a = 24.43174 (26) Å, b = 13.90230 (7) Å, c = 12.28142 (8) Å and a monoclinic angle of 108.9693 (21)° with a space group C 2/m. Bond angle and distance restraints in final refinement were weighted by a factor of 0.8 (Rp=3.88 %, Rwp=6.50 %, RF^2=7.51 %).

T atom Name	x coordinate	y coordinate	z coordinate	Uiso	Site Multiplicity
Si3	0.30497(18)	0.79769(26)	0.24374(32)	0.0436(19)	8
Si4	0.31078(11)	0.79710(22)	0.50510(32)	0.0191(18)	8
Si5	0.31763(18)	0.79183(22)	0.87041(34)	0.0240(19)	8
Si6	0.37557(20)	0.70222(28)	0.1090(4)	0.0180(29)	8
Si7	0.38626(24)	0.69952(27)	0.72787(34)	0.03(5)	8
Si8	0.26705(24)	0	0.7980(4)	0.0500(29)	4
Si9	0.22261(22)	0.5	0.8158(5)	0.094(4)	4
Si10	0.31731(21)	0.5	0.6875(4)	0.0072(23)	4
Si11	0.22771(24)	0.5	0.4548(5)	0.0312(28)	4
Si12	0.31173(24)	0.5	0.0702(5)	0.038(4)	4
Si13	-0.0143(6)	0.8899(4)	0.1130(18)	0.081(2)	8
O1	0.31868(20)	0.90691(23)	0.2176(5)	0.034(4)	8
O2	0.35238(29)	0.7330(5)	0.2127(5)	0.046(6)	8
O3	0.31715(30)	0.7852(4)	0.37968(34)	0.0140(31)	8
O4	0.23872(20)	0.7742(4)	0.1752(6)	0.0111(32)	8
O5	0.31138(26)	0.90869(25)	0.5384(7)	0.0265(8)	8
O6	0.25	0.75	0.5	0.025(5)	4
O7	0.36249(22)	0.7409(4)	0.5983(4)	0.0109(33)	8
O8	0.33252(32)	0.7609(5)	0.0024(4)	0.022(4)	8
O9	0.30313(23)	0.90450(23)	0.8502(5)	0.0030(29)	8
O10	0.36651(31)	0.7674(5)	0.8143(7)	0.109(6)	8
O11	0.35236(26)	0.59327(27)	0.0844(6)	0.067(5)	8
O13	0.35651(23)	0.59524(25)	0.7226(5)	0.0080(33)	8
O14	0.20415(30)	0	0.8130(6)	0.076(7)	4
O15	0.25586(35)	0	0.6615(5)	0.007(4)	4
O16	0.25856(30)	0.5	0.9515(5)	0.0314(32)	4
O17	0.2643(4)	0.5	0.7380(10)	0.066(26)	4
O18	0.29114(30)	0.5	0.5493(4)	0.012(5)	4
Oa	0.94453(21)	0.8127(6)	0.1456(8)	0.0538(30)	8

DOI: 10.1038/NMAT3455

Ob	0	0.1401(13)	0	0.048(7)	4
Oc	-0.0356(10)	0	0.1060(22)	0.038(17)	4
Od	0.04572(31)	0.8195(10)	0.2077(15)	0.028(7)	8
Si'13	-0.0104(4)	0.8875(6)	0.1591(20)	0.047(3)	8
O'a	0.9400(15)	0.9024(28)	0.2218(31)	0.096(5)	8
O'c	0.0152(15)	0	0.146(4)	0.094(4)	4
O'd	0.0488(5)	0.8760(15)	0.1886(28)	0.0411(3)	8
Si'6	0.3761(4)	0.7022(6)	0.1069(8)	0.1050(3)	8
Si'7	0.38567(24)	0.69955(27)	0.72746(34)	0.0831(5)	8
ge1	0.0143(4)	0.6135(4)	0.1328(10)	0.0764(5)	8
ge2	-0.0208(6)	0.6088(5)	0.1234(12)	0.0957(3)	8
O41	-0.0079(11)	0.5	0.8114(5)	0.0337(3)	4
O48	0.0460(18)	0.6284(8)	0.0252(18)	0.0914(7)	8
O47	0.0504(8)	0.6393(4)	0.2034(5)	0.0391(5)	8
O44	-0.0514(14)	0.6430(4)	0.1519(5)	0.0891(2)	8
Og48	0.0210(15)	0.4670(30)	-0.0206(4)	0.0129(7)	8
Og43	0.0621(4)	0.6985(8)	0.2312(11)	0.0218(3)	8
Og49	-0.0628(11)	0.7199(11)	0.1164(4)	0.0233(6)	8
Og50	-0.0697(11)	0.525(2)	0.1378(7)	0.0946(4)	8
Ow1	0.0501(4)	0.2436(4)	0.4973(8)	0.025	8
Ow2	0.9859(7)	0.2124(10)	0.3793(11)	0.025	8
Ow3	0.9601(4)	0.5	0.304(1)	0.025	4
Ow4	0.0503(7)	0.5	0.3323(12)	0.025	4

P1 representation, derived from Rietveld in C 2/m

Table S14: Atomic coordinates of the Ge-COK-14 structure in P1 with a unit cell doubled along b. a = 24.4317 (6) Å, b = 27.80460 (15) Å, c = 12.28140 (19) Å α = 90 °, β = 108.9690 (16)° and γ = 90 °. Coordinates were obtained by lowering the symmetry of C2/m to P1 to avoid split atomic positions.

T atom Name	x coordinate	y coordinate	z coordinate	Uiso	Site Multiplicity
Si3	0.30497	0.39884	0.24374	1	1
Si3	0.69503	0.39884	0.75626	1	1
Si3	0.69503	0.10115	0.75626	1	1
Si3	0.30497	0.10115	0.24374	1	1
Si4	0.31078	0.39855	0.5051	1	1
Si4	0.68922	0.39855	0.4949	1	1
Si4	0.68922	0.10145	0.4949	1	1
Si4	0.31078	0.10145	0.5051	1	1
Si5	0.31763	0.39592	0.87041	1	1
Si5	0.68237	0.39592	0.12959	1	1
Si5	0.68237	0.10408	0.12959	1	1
Si5	0.31763	0.10408	0.87041	1	1
Si6	0.37557	0.35111	0.109	1	1
Si6	0.37557	0.14889	0.109	1	1
Si7	0.38626	0.34976	0.72787	1	1
Si7	0.38626	0.15024	0.72787	1	1
Si8	0.26705	0	0.798	1	1
Si8	0.73295	0	0.202	1	1
Si9	0.22261	0.25	0.8158	1	1
Si9	0.77739	0.25	0.1842	1	1
Si10	0.31731	0.25	0.6875	1	1
Si10	0.68269	0.25	0.3125	1	1
Si11	0.22771	0.25	0.4548	1	1
Si11	0.77229	0.25	0.5452	1	1
Si12	0.31173	0.25	0.0702	1	1
Si12	0.68827	0.25	0.9298	1	1
O1	0.31868	0.45346	0.2176	1	1
O1	0.68132	0.45346	0.7824	1	1
O1	0.68132	0.04654	0.7824	1	1
O1	0.31868	0.04654	0.2176	1	1
O2	0.35238	0.3665	0.2127	1	1
O2	0.64762	0.3665	0.7873	1	1
O2	0.64762	0.1335	0.7873	1	1
O2	0.35238	0.1335	0.2127	1	1
O3	0.31715	0.3926	0.37968	1	1
O3	0.68285	0.3926	0.62032	1	1
O3	0.68285	0.1074	0.62032	1	1
O3	0.31715	0.1074	0.37968	1	1
O4	0.23872	0.3871	0.1752	1	1
O4	0.76128	0.3871	0.8248	1	1
O4	0.76128	0.1129	0.8248	1	1
O4	0.23872	0.1129	0.1752	1	1
O5	0.31138	0.45434	0.5384	1	1
O5	0.68862	0.45434	0.4616	1	1
O5	0.68862	0.04566	0.4616	1	1

DOI: 10.1038/NMAT3455

O5	0.31138	0.04566	0.5384	1	1
O6	0.25	0.375	0.5	1	1
O6	0.75	0.375	0.5	1	1
O7	0.36249	0.37045	0.5983	1	1
O7	0.63751	0.37045	0.4017	1	1
O7	0.13751	0.12045	0.4017	1	1
O7	0.63751	0.12955	0.4017	1	1
O7	0.13751	0.37955	0.4017	1	1
O7	0.36249	0.12955	0.5983	1	1
O7	0.86249	0.37955	0.5983	1	1
O8	0.33252	0.38045	0.0024	1	1
O8	0.83252	0.13045	0.0024	1	1
O8	0.66748	0.38045	0.9976	1	1
O8	0.16748	0.13045	0.9976	1	1
O8	0.66748	0.11955	0.9976	1	1
O8	0.16748	0.36955	0.9976	1	1
O8	0.33252	0.11955	0.0024	1	1
O8	0.83252	0.36955	0.0024	1	1
O9	0.30313	0.45225	0.8502	1	1
O9	0.80313	0.20225	0.8502	1	1
O9	0.69687	0.45225	0.1498	1	1
O9	0.19687	0.20225	0.1498	1	1
O9	0.69687	0.04775	0.1498	1	1
O9	0.19687	0.29775	0.1498	1	1
O9	0.30313	0.04775	0.8502	1	1
O9	0.80313	0.29775	0.8502	1	1
O10	0.36651	0.3837	0.8143	1	1
O10	0.86651	0.1337	0.8143	1	1
O10	0.63349	0.3837	0.1857	1	1
O10	0.13349	0.1337	0.1857	1	1
O10	0.63349	0.1163	0.1857	1	1
O10	0.13349	0.3663	0.1857	1	1
O10	0.36651	0.1163	0.8143	1	1
O10	0.86651	0.3663	0.8143	1	1
O11	0.35236	0.29664	0.0844	1	1
O11	0.85236	0.04663	0.0844	1	1
O11	0.64764	0.29664	0.9156	1	1
O11	0.14764	0.04663	0.9156	1	1
O11	0.64764	0.20336	0.9156	1	1
O11	0.14764	0.45336	0.9156	1	1
O11	0.35236	0.20336	0.0844	1	1
O11	0.85236	0.45336	0.0844	1	1
O13	0.35651	0.29762	0.7226	1	1
O13	0.85651	0.04762	0.7226	1	1
O13	0.64349	0.29762	0.2774	1	1
O13	0.14349	0.04762	0.2774	1	1
O13	0.64349	0.20238	0.2774	1	1
O13	0.14349	0.45238	0.2774	1	1
O13	0.35651	0.20238	0.7226	1	1
O13	0.85651	0.45238	0.7226	1	1
O14	0.20415	0	0.813	1	1
O14	0.70415	0.25	0.813	1	1
O14	0.79585	0	0.187	1	1
O14	0.29585	0.25	0.187	1	1
O15	0.25586	0	0.6615	1	1
O15	0.75586	0.25	0.6615	1	1

O15	0.74414	0	0.3385	1	1
O15	0.24414	0.25	0.3385	1	1
O16	0.25856	0.25	0.9515	1	1
O16	0.75856	0	0.9515	1	1
O16	0.74144	0.25	0.0485	1	1
O16	0.24144	0	0.0485	1	1
O17	0.2643	0.25	0.738	1	1
O17	0.7643	0	0.738	1	1
O17	0.7357	0.25	0.262	1	1
O17	0.2357	0	0.262	1	1
O18	0.29114	0.25	0.5493	1	1
O18	0.79114	0	0.5493	1	1
O18	0.70886	0.25	0.4507	1	1
O18	0.20886	0	0.4507	1	1
Si13	0.9857	0.44495	0.113	1	1
Si13	0.4857	0.19495	0.113	1	1
Si13	0.0143	0.05505	0.887	1	1
Si13	0.4857	0.30505	0.113	1	1
Oa	0.94453	0.40635	0.1456	1	1
Oa	0.44453	0.15635	0.1456	1	1
Oa	0.05547	0.09365	0.8544	1	1
Oa	0.44453	0.34365	0.1456	1	1
Ob	0	0.07005	0	1	1
Ob	0.5	0.32005	0	1	1
Ob	0	0.42995	0	1	1
Ob	0.5	0.17995	0	1	1
Oc	0.4644	0.25	0.106	1	1
Oc	0.0356	0	0.894	1	1
Od	0.95428	0.40975	0.7923	1	1
Od	0.45428	0.15975	0.7923	1	1
Od	0.45428	0.34025	0.7923	1	1
Od	0.04572	0.09025	0.2077	1	1
Si'13	0.0104	0.44375	0.8409	1	1
Si'13	0.5104	0.19375	0.8409	1	1
Si'13	0.5104	0.30625	0.8409	1	1
Si'13	0.9896	0.05625	0.1591	1	1
O'a	0.06	0.4512	0.7782	1	1
O'a	0.56	0.2012	0.7782	1	1
O'a	0.56	0.2988	0.7782	1	1
O'a	0.94	0.0488	0.2218	1	1
O'c	0.0152	0	0.146	1	1
O'c	0.4848	0.25	0.854	1	1
O'd	0.0488	0.438	0.1886	1	1
O'd	0.5488	0.188	0.1886	1	1
O'd	0.9512	0.062	0.8114	1	1
O'd	0.5488	0.312	0.1886	1	1
Si'6	0.8761	0.1011	0.1069	1	1
Si'6	0.6239	0.3511	0.8931	1	1
Si'6	0.6239	0.1489	0.8931	1	1
Si'6	0.1239	0.3989	0.8931	1	1
Si'6	0.3761	0.1489	0.1069	1	1
Si'7	0.88567	0.09978	0.72746	1	1
Si'7	0.61433	0.34977	0.27254	1	1
Si'7	0.61433	0.15022	0.27254	1	1
Si'7	0.11433	0.40023	0.27254	1	1
ge1	0.0143	0.30675	0.1328	1	1

DOI: 10.1038/NMAT3455

ge1	0.5143	0.05675	0.1328	1	1
ge1	0.9857	0.19325	0.8672	1	1
ge1	0.5143	0.44325	0.1328	1	1
ge2	0.0208	0.3044	0.8766	1	1
ge2	0.5208	0.0544	0.8766	1	1
ge2	0.5208	0.4456	0.8766	1	1
ge2	0.9792	0.1956	0.1234	1	1
O41	0.9921	0.25	0.8114	1	1
O41	0.4921	0	0.8114	1	1
O41	0.0079	0.25	0.1886	1	1
O41	0.5079	0	0.1886	1	1
O48	0.046	0.3142	0.0252	1	1
O48	0.546	0.0642	0.0252	1	1
O48	0.954	0.1858	0.9748	1	1
O48	0.546	0.4358	0.0252	1	1
O47	0.9496	0.31965	0.7966	1	1
O47	0.4496	0.06965	0.7966	1	1
O47	0.4496	0.43035	0.7966	1	1
O47	0.0504	0.18035	0.2034	1	1
O44	0.9486	0.3215	0.1519	1	1
O44	0.4486	0.0715	0.1519	1	1
O44	0.0514	0.1785	0.8481	1	1
O44	0.4486	0.4285	0.1519	1	1
Og48	0.021	0.2335	0.9794	1	1
Og48	0.479	0.4835	0.0206	1	1
Og43	0.0621	0.34925	0.2312	1	1
Og43	0.5621	0.09925	0.2312	1	1
Og43	0.9379	0.15075	0.7688	1	1
Og43	0.5621	0.40075	0.2312	1	1
Og49	0.0628	0.35995	0.8836	1	1
Og49	0.5628	0.10995	0.8836	1	1
Og49	0.5628	0.39005	0.8836	1	1
Og49	0.9372	0.14005	0.1164	1	1
Og50	0.0697	0.2625	0.8622	1	1
Og50	0.5697	0.0125	0.8622	1	1
Og50	0.5697	0.4875	0.8622	1	1
Og50	0.9303	0.2375	0.1378	1	1
Ow1	0.0501	0.1218	0.4973	1	1
Ow1	0.5501	0.3718	0.4973	1	1
Ow1	0.9499	0.1218	0.5027	1	1
Ow1	0.4499	0.3718	0.5027	1	1
Ow1	0.9499	0.3782	0.5027	1	1
Ow1	0.4499	0.1282	0.5027	1	1
Ow1	0.0501	0.3782	0.4973	1	1
Ow1	0.5501	0.1282	0.4973	1	1
Ow2	0.9859	0.1062	0.3793	1	1
Ow2	0.4859	0.3562	0.3793	1	1
Ow2	0.0141	0.1062	0.6207	1	1
Ow2	0.5141	0.3562	0.6207	1	1
Ow2	0.0141	0.3938	0.6207	1	1
Ow2	0.5141	0.1438	0.6207	1	1
Ow2	0.9859	0.3938	0.3793	1	1
Ow2	0.4859	0.1438	0.3793	1	1
Ow3	0.9601	0.25	0.3042	1	1
Ow3	0.4601	0	0.3042	1	1
Ow3	0.0399	0.25	0.6958	1	1

Ow3	0.5399	0	0.6958	1	1
Ow4	0.0503	0.25	0.3323	1	1
Ow4	0.5503	0	0.3323	1	1
Ow4	0.9497	0.25	0.6677	1	1
Ow4	0.4497	0	0.6677	1	1
Si3	0.30497	0.89885	0.24374	1	1
Si3	0.80497	0.64885	0.24374	1	1
Si3	0.69503	0.89885	0.75626	1	1
Si3	0.19503	0.64885	0.75626	1	1
Si3	0.69503	0.60115	0.75626	1	1
Si3	0.19503	0.85115	0.75626	1	1
Si3	0.30497	0.60115	0.24374	1	1
Si3	0.80497	0.85115	0.24374	1	1
Si4	0.31078	0.89855	0.5051	1	1
Si4	0.81078	0.64855	0.5051	1	1
Si4	0.68922	0.89855	0.4949	1	1
Si4	0.18922	0.64855	0.4949	1	1
Si4	0.68922	0.60145	0.4949	1	1
Si4	0.18922	0.85145	0.4949	1	1
Si4	0.31078	0.60145	0.5051	1	1
Si4	0.81078	0.85145	0.5051	1	1
Si5	0.31763	0.89591	0.87041	1	1
Si5	0.81763	0.64591	0.87041	1	1
Si5	0.68237	0.89591	0.12959	1	1
Si5	0.18237	0.64591	0.12959	1	1
Si5	0.68237	0.60409	0.12959	1	1
Si5	0.18237	0.85409	0.12959	1	1
Si5	0.31763	0.60409	0.87041	1	1
Si5	0.81763	0.85409	0.87041	1	1
Si6	0.87557	0.60111	0.109	1	1
Si6	0.62443	0.85111	0.891	1	1
Si6	0.62443	0.64889	0.891	1	1
Si6	0.12443	0.89889	0.891	1	1
Si7	0.88626	0.59976	0.72787	1	1
Si7	0.61374	0.84976	0.27213	1	1
Si7	0.61374	0.65024	0.27213	1	1
Si7	0.11374	0.90024	0.27213	1	1
Si8	0.26705	0.5	0.798	1	1
Si8	0.76705	0.75	0.798	1	1
Si8	0.73295	0.5	0.202	1	1
Si8	0.23295	0.75	0.202	1	1
Si9	0.22261	0.75	0.8158	1	1
Si9	0.72261	0.5	0.8158	1	1
Si9	0.77739	0.75	0.1842	1	1
Si9	0.27739	0.5	0.1842	1	1
Si10	0.31731	0.75	0.6875	1	1
Si10	0.81731	0.5	0.6875	1	1
Si10	0.68269	0.75	0.3125	1	1
Si10	0.18269	0.5	0.3125	1	1
Si11	0.22771	0.75	0.4548	1	1
Si11	0.72771	0.5	0.4548	1	1
Si11	0.77229	0.75	0.5452	1	1
Si11	0.27229	0.5	0.5452	1	1
Si12	0.31173	0.75	0.0702	1	1
Si12	0.81173	0.5	0.0702	1	1
Si12	0.68827	0.75	0.9298	1	1

DOI: 10.1038/NMAT3455

Si12	0.18827	0.5	0.9298	1	1
O1	0.31868	0.95345	0.2176	1	1
O1	0.81868	0.70345	0.2176	1	1
O1	0.68132	0.95345	0.7824	1	1
O1	0.18132	0.70345	0.7824	1	1
O1	0.68132	0.54655	0.7824	1	1
O1	0.18132	0.79655	0.7824	1	1
O1	0.31868	0.54655	0.2176	1	1
O1	0.81868	0.79655	0.2176	1	1
O2	0.35238	0.8665	0.2127	1	1
O2	0.85238	0.6165	0.2127	1	1
O2	0.64762	0.8665	0.7873	1	1
O2	0.14762	0.6165	0.7873	1	1
O2	0.64762	0.6335	0.7873	1	1
O2	0.14762	0.8835	0.7873	1	1
O2	0.35238	0.6335	0.2127	1	1
O2	0.85238	0.8835	0.2127	1	1
O3	0.31715	0.8926	0.37968	1	1
O3	0.81715	0.6426	0.37968	1	1
O3	0.68285	0.8926	0.62032	1	1
O3	0.18285	0.6426	0.62032	1	1
O3	0.68285	0.6074	0.62032	1	1
O3	0.18285	0.8574	0.62032	1	1
O3	0.31715	0.6074	0.37968	1	1
O3	0.81715	0.8574	0.37968	1	1
O4	0.23872	0.8871	0.1752	1	1
O4	0.73872	0.6371	0.1752	1	1
O4	0.76128	0.8871	0.8248	1	1
O4	0.26128	0.6371	0.8248	1	1
O4	0.76128	0.6129	0.8248	1	1
O4	0.26128	0.8629	0.8248	1	1
O4	0.23872	0.6129	0.1752	1	1
O4	0.73872	0.8629	0.1752	1	1
O5	0.31138	0.95434	0.5384	1	1
O5	0.81138	0.70434	0.5384	1	1
O5	0.68862	0.95434	0.4616	1	1
O5	0.18862	0.70434	0.4616	1	1
O5	0.68862	0.54566	0.4616	1	1
O5	0.18862	0.79566	0.4616	1	1
O5	0.31138	0.54566	0.5384	1	1
O5	0.81138	0.79566	0.5384	1	1
O6	0.25	0.875	0.5	1	1
O6	0.75	0.625	0.5	1	1
O6	0.75	0.875	0.5	1	1
O6	0.25	0.625	0.5	1	1
O7	0.36249	0.87045	0.5983	1	1
O7	0.86249	0.62045	0.5983	1	1
O7	0.63751	0.87045	0.4017	1	1
O7	0.13751	0.62045	0.4017	1	1
O7	0.63751	0.62955	0.4017	1	1
O7	0.13751	0.87955	0.4017	1	1
O7	0.36249	0.62955	0.5983	1	1
O7	0.86249	0.87955	0.5983	1	1
O8	0.33252	0.88045	0.0024	1	1
O8	0.83252	0.63045	0.0024	1	1
O8	0.66748	0.88045	0.9976	1	1

O8	0.16748	0.63045	0.9976	1	1
O8	0.66748	0.61955	0.9976	1	1
O8	0.16748	0.86955	0.9976	1	1
O8	0.33252	0.61955	0.0024	1	1
O8	0.83252	0.86955	0.0024	1	1
O9	0.30313	0.95225	0.8502	1	1
O9	0.80313	0.70225	0.8502	1	1
O9	0.69687	0.95225	0.1498	1	1
O9	0.19687	0.70225	0.1498	1	1
O9	0.69687	0.54775	0.1498	1	1
O9	0.19687	0.79775	0.1498	1	1
O9	0.30313	0.54775	0.8502	1	1
O9	0.80313	0.79775	0.8502	1	1
O10	0.36651	0.8837	0.8143	1	1
O10	0.86651	0.6337	0.8143	1	1
O10	0.63349	0.8837	0.1857	1	1
O10	0.13349	0.6337	0.1857	1	1
O10	0.63349	0.6163	0.1857	1	1
O10	0.13349	0.8663	0.1857	1	1
O10	0.36651	0.6163	0.8143	1	1
O10	0.86651	0.8663	0.8143	1	1
O11	0.35236	0.79663	0.0844	1	1
O11	0.85236	0.54663	0.0844	1	1
O11	0.64764	0.79663	0.9156	1	1
O11	0.14764	0.54663	0.9156	1	1
O11	0.64764	0.70337	0.9156	1	1
O11	0.14764	0.95337	0.9156	1	1
O11	0.35236	0.70337	0.0844	1	1
O11	0.85236	0.95337	0.0844	1	1
O13	0.35651	0.79762	0.7226	1	1
O13	0.85651	0.54762	0.7226	1	1
O13	0.64349	0.79762	0.2774	1	1
O13	0.14349	0.54762	0.2774	1	1
O13	0.64349	0.70238	0.2774	1	1
O13	0.14349	0.95238	0.2774	1	1
O13	0.35651	0.70238	0.7226	1	1
O13	0.85651	0.95238	0.7226	1	1
O14	0.20415	0.5	0.813	1	1
O14	0.70415	0.75	0.813	1	1
O14	0.79585	0.5	0.187	1	1
O14	0.29585	0.75	0.187	1	1
O15	0.25586	0.5	0.6615	1	1
O15	0.75586	0.75	0.6615	1	1
O15	0.74414	0.5	0.3385	1	1
O15	0.24414	0.75	0.3385	1	1
O16	0.25856	0.75	0.9515	1	1
O16	0.75856	0.5	0.9515	1	1
O16	0.74144	0.75	0.0485	1	1
O16	0.24144	0.5	0.0485	1	1
O17	0.2643	0.75	0.738	1	1
O17	0.7643	0.5	0.738	1	1
O17	0.7357	0.75	0.262	1	1
O17	0.2357	0.5	0.262	1	1
O18	0.29114	0.75	0.5493	1	1
O18	0.79114	0.5	0.5493	1	1
O18	0.70886	0.75	0.4507	1	1

DOI: 10.1038/NMAT3455

O18	0.20886	0.5	0.4507	1	1
Si13	0.5143	0.69495	0.887	1	1
Si13	0.0143	0.94495	0.887	1	1
Si13	0.9857	0.55505	0.113	1	1
Si13	0.5143	0.80505	0.887	1	1
Oa	0.05547	0.90635	0.8544	1	1
Oa	0.55547	0.65635	0.8544	1	1
Oa	0.55547	0.84365	0.8544	1	1
Oa	0.94453	0.59365	0.1456	1	1
Ob	0	0.57005	0	1	1
Ob	0.5	0.82005	0	1	1
Ob	0	0.92995	0	1	1
Ob	0.5	0.67995	0	1	1
Oc	0.9644	0.5	0.106	1	1
Oc	0.5356	0.75	0.894	1	1
Od	0.04572	0.90975	0.2077	1	1
Od	0.54572	0.65975	0.2077	1	1
Od	0.95428	0.59025	0.7923	1	1
Od	0.54572	0.84025	0.2077	1	1
Si'13	0.9896	0.94375	0.1591	1	1
Si'13	0.4896	0.69375	0.1591	1	1
Si'13	0.0104	0.55625	0.8409	1	1
Si'13	0.4896	0.80625	0.1591	1	1
O'a	0.94	0.9512	0.2218	1	1
O'a	0.44	0.7012	0.2218	1	1
O'a	0.06	0.5488	0.7782	1	1
O'a	0.44	0.7988	0.2218	1	1
O'c	0.9848	0.5	0.854	1	1
O'c	0.5152	0.75	0.146	1	1
O'd	0.9512	0.938	0.8114	1	1
O'd	0.4512	0.688	0.8114	1	1
O'd	0.4512	0.812	0.8114	1	1
O'd	0.0488	0.562	0.1886	1	1
Si'6	0.3761	0.8511	0.1069	1	1
Si'6	0.1239	0.6011	0.8931	1	1
Si'6	0.3761	0.6489	0.1069	1	1
Si'6	0.8761	0.8989	0.1069	1	1
Si'7	0.38567	0.84978	0.72746	1	1
Si'7	0.11433	0.59978	0.27254	1	1
Si'7	0.38567	0.65022	0.72746	1	1
Si'7	0.88567	0.90022	0.72746	1	1
ge1	0.9857	0.80675	0.8672	1	1
ge1	0.4857	0.55675	0.8672	1	1
ge1	0.4857	0.94325	0.8672	1	1
ge1	0.0143	0.69325	0.1328	1	1
ge2	0.9792	0.8044	0.1234	1	1
ge2	0.4792	0.5544	0.1234	1	1
ge2	0.0208	0.6956	0.8766	1	1
ge2	0.4792	0.9456	0.1234	1	1
O41	0.9921	0.75	0.8114	1	1
O41	0.4921	0.5	0.8114	1	1
O41	0.0079	0.75	0.1886	1	1
O41	0.5079	0.5	0.1886	1	1
O48	0.546	0.5642	0.0252	1	1
O48	0.954	0.8142	0.9748	1	1
O48	0.454	0.5642	0.9748	1	1

O48	0.454	0.9358	0.9748	1	1
O48	0.046	0.6858	0.0252	1	1
O47	0.0504	0.81965	0.2034	1	1
O47	0.5504	0.56965	0.2034	1	1
O47	0.9496	0.68035	0.7966	1	1
O47	0.5504	0.93035	0.2034	1	1
O44	0.0514	0.8215	0.8481	1	1
O44	0.5514	0.9285	0.8481	1	1
O44	0.9486	0.6785	0.1519	1	1
Og48	0.521	0.9835	0.9794	1	1
Og48	0.021	0.7665	0.9794	1	1
Og43	0.9379	0.84925	0.7688	1	1
Og43	0.4379	0.59925	0.7688	1	1
Og43	0.4379	0.90075	0.7688	1	1
Og43	0.0621	0.65075	0.2312	1	1
Og49	0.9372	0.85995	0.1164	1	1
Og49	0.4372	0.60995	0.1164	1	1
Og49	0.0628	0.64005	0.8836	1	1
Og49	0.4372	0.89005	0.1164	1	1
Og50	0.9303	0.7625	0.1378	1	1
Og50	0.4303	0.5125	0.1378	1	1
Og50	0.0697	0.7375	0.8622	1	1
Og50	0.4303	0.9875	0.1378	1	1
Ow1	0.0501	0.6218	0.4973	1	1
Ow1	0.5501	0.8718	0.4973	1	1
Ow1	0.9499	0.6218	0.5027	1	1
Ow1	0.4499	0.8718	0.5027	1	1
Ow1	0.9499	0.8782	0.5027	1	1
Ow1	0.4499	0.6282	0.5027	1	1
Ow1	0.0501	0.8782	0.4973	1	1
Ow1	0.5501	0.6282	0.4973	1	1
Ow2	0.9859	0.6062	0.3793	1	1
Ow2	0.4859	0.8562	0.3793	1	1
Ow2	0.0141	0.6062	0.6207	1	1
Ow2	0.5141	0.8562	0.6207	1	1
Ow2	0.0141	0.8938	0.6207	1	1
Ow2	0.5141	0.6438	0.6207	1	1
Ow2	0.9859	0.8938	0.3793	1	1
Ow2	0.4859	0.6438	0.3793	1	1
Ow3	0.9601	0.75	0.3042	1	1
Ow3	0.4601	0.5	0.3042	1	1
Ow3	0.0399	0.75	0.6958	1	1
Ow3	0.5399	0.5	0.6958	1	1
Ow4	0.0503	0.75	0.3323	1	1
Ow4	0.5503	0.5	0.3323	1	1
Ow4	0.9497	0.75	0.6677	1	1
Ow4	0.4497	0.5	0.6677	1	1

DOI: 10.1038/NMAT3455

References

1 Shvets, O. V., Zukal, A., Kasian, N., Žilková, N. & Čejka, J. The role of crystallization parameters for the synthesis of germanosilicate with UTL topology. *Chem. Eur. J.* **14,** 10134-10140 (2008).

2 Knapp, M., Baehtz, C., Ehrenberg, H. & Fuess, H. The synchrotron powder diffractometer at beamline B2 at HASYLAB/DESY: status and capabilities. *J. Synchrotron Radiat.* **11,** 328-334 (2004).

3 Knapp *et al.* Position-sensitive detector system OBI for High Resolution X-Ray Powder Diffraction using on-site readable image plates. *Nucl. Instrum. Methods Phys. Res. A* **521,** 565-570 (2004).

4 Van Beek, W., Safonova, O. V., Wiker, G., Emerich, H. SNBL, a dedicated beamline for combined in situ X-ray diffraction, X-ray absorption and Raman scattering experiments. *Phase Transition*s **84,** 726-732 (2011).

5 Larson, A. C. & Von Dreele, R. B. General structure analysis system (GSAS). *Los Alamos National Laboratory Report LAUR* 86-748 (2004).

6 Toby, B. H., EXPGUI, a graphical user interface for GSAS. *J. Appl. Crystallogr.* ***34*****,** 210–213 (2001).

7 Nikitenko *et al.* Implementation of a combined SAXS/WAXS/QEXAFS set-up for time-resolved insituexperiments. *J. Synchotron Radiat.* **15,** 632-640 (2008).

8 Ravel B., Newville, M., Athena, artemis, hephaestus: data analysis for X-ray absorption spectroscopy using IFEFFIT. *J. Synchotron Radiat.* **12,** 537-541 (2005).

9 Newville, M. EXAFS analysis using FEFF and FEFFIT. *J. Synchotron Radiat*. **8,** 96-100 (2001).

10 Ravel, B. A comprehensive system for processing and analyzing X-ray absorption spectroscopy. http://bruceravel.github.com/demeter/

11 Rehr J. J., & Albers, R. C. Theoretical approaches to X-ray absorption fine structure. *Rev. Mod. Phys.* **72**, 621-654 (2000).

12 Kline, S. R., Reduction and analysis of SANS and USANS data using IGOR Pro. *J. Appl. Cryst.* **39,** 895-900 (2006).

13 Vinogradov, E., Madhu, P. K. & Vega, S. High-resolution proton solid-state NMR spectroscopy by phase-modulated Lee-Goldburg experiment. *Chem. Phys. Lett.* **314,** 443-450 (1999).

14 Leskes, M., Madhu, P. K. & Vega, S. Proton line narrowing in solid-state nuclear magnetic resonance: new insights from windowed phase-modulated Lee-Goldburg sequence. *J. Chem. Phys.* **125,** 124506-12450623 (2006).

15 Leskes, M., Madhu, P. K. & Vega, S. A broad-banded z-rotation windowed phase-modulated Lee-Goldburg pulse sequence for ^{1}H spectroscopy in solid-state NMR. *Chem. Phys. Lett.* **447,** 370-374 (2007).

16 Massiot *et al*. Modelling one- and two-dimensional solid-state NMR spectra. *Magn. Reson. Chem.* **40,** 70-76 (2002).

17 Saito, A & Foley, H. C. Curvature and parametric sensitivity in models for adsorption in micropores. *AIChe J.* **37,** 429–436 (1991).

18 Gale, J. D. GULP : A computer program for the symmetry-adapted simulation of solids. *J. Chem. Soc., Faraday Trans.* **93**, 629-637 (1997).

19 Schroder, K. P., Sauer, J., Leslie, M., Catlow, C. R. A. & Thomas, J. M. Bridging hydroxyl-groups in zeolite catalysis – a computer-simulation of their structure, vibrational properties and acidity in protonated faujasites (H-Y zeolites). *Chem. Phys. Lett.* **188,** 320-325 (1992).

20 Kresse, G. & Furthmüller, J. Efficiency of ab-initio total energy calculations for metals and semiconductors using a plane-wave basis set. *Comput. Mat. Sci* **6,** 15-50 (1996).

21 Kresse, G. & Furthmüller, J. Efficient iterative schemes for ab initio total-energy calculations using a plane-wave basis set. *Phys. Rev. B* **54,** 11169-11186 (1996).

22 Grimme, S. Accurate description of van der Waals complexes by density functional theory including empirical correction. *J. Comput. Chem.* **25,** 1463-1473 (2004).

23 Baerlocher C., McCusker, L. B. & Olson, D. H. *Atlas of Zeolite Framework Types* (Elsevier, Amsterdam, 2007).

24 CIF files may be obtained from Fachinformationszentrum Karlsruhe (crysdata@fiz-karlsruhe.de). CSD number 424470 refers to partially dried -COK-14 zeolite recorded on a STOE Stadi MP diffractometer (Rp=3.20 %, Rwp=4.50 %, RF^2=11.35 %) and 424471 to the structure equilibrated at ambient conditions recorded with synchrotron radiation ((Rp=2.60 %, Rwp=3.31 %, RF^2=8.77 %).

25 Jiang, Y., Huang, J., Dai, W., & Hunger, M. Solid-state nuclear magnetic resonance investigations of the nature, property, and activity of acid sites on solid catalysts. *Solid State Nucl. Magn. Reson.*, **39,** 116–141 (2011).

26 Roth *et al.* Postsynthesis transformation of three-dimensional framework into a lamellar zeolite with modifiable architecture. *J. Am. Chem. Soc.* **133,** 6130-6133 (2011).

27 Bolis *et al.* Calorimetric and IR spectroscopic study of the interaction of NH_3 with variously prepared defective silicalites. Comparison with ab initio computational data. *Appl. Surf. Sci.* **196,** 56-70 (2002).

28 Li, H. Eddaoudi, M. & Yaghi, O. M. An open-framework germanate with polycubane-like topology. *Angew. Chem. Int. Ed.* **38,** 653-655 (1999).

29 Christensen *et al.* Design of open-framework germanates by combining different building units. *J. Am. Chem. Soc.* **128,** 14238-14239 (2006).

30 Paillaud, J., Harbuzaru, B., Patarin, J. & Bats, N. Extra-large-pore zeolites with two-dimensional channels formed by 14 and 12 rings. *Science* **304,** 990-992 (2004).